IEEE Access
Multidisciplinary ⋮ Rapid Review ⋮ Open Access Journal

Received 25 January 2023, accepted 13 March 2023, date of publication 22 March 2023, date of current version 31 March 2023.

Digital Object Identifier 10.1109/ACCESS.2023.3260768

SURVEY

A Comprehensive Review of Harmonic Issues and Estimation Techniques in Power System Networks Based on Traditional and Artificial Intelligence/Machine Learning

AMIR TAGHVAIE[1], (Member, IEEE), T. WARNAKULASURIYA[1], (Member, IEEE), DINESH KUMAR[2], (Senior Member, IEEE), FIRUZ ZARE[1], (Fellow, IEEE), RAHUL SHARMA[3], (Senior Member, IEEE), AND D. MAHINDA VILATHGAMUWA[1], (Fellow, IEEE)

[1]School of Electrical Engineering and Robotics, Queensland University of Technology, Brisbane, QLD 4000, Australia
[2]Global Research and Development Center, Danfoss Drives A/S, 6300 Grasten, Denmark
[3]School of Information Technology and Electrical Engineering, The University of Queensland, Brisbane, QLD 4072, Australia

Corresponding author: Amir Taghvaie (taghvaia@qut.edu.au)

ABSTRACT Modern industrial and commercial devices that are fed by power electronics circuits and behave non-linearly tend to produce power quality issues in power systems including harmonics and interharmonics, swell, flicker, spikes, notches, and transient instabilities. Among them, harmonic emission is the most significant challenge to be overcome by the distribution networks. Unwanted current, overheating motors and transformers, equipment failure, and circuit breaker misoperation are some of the harmonic consequences. While it is important to employ the best methods to mitigate or suppress the harmonic distortions in power systems, it is even more essential to estimate these harmonics at the outset by developing smart, efficient, and accurate techniques. Due to their capability for learning, predicting, and identifying, researchers have turned to Artificial Intelligence technologies for harmonic estimation in distribution networks. Although the power system parameters (impedance/admittance model) and many harmonic monitors are prerequisites for traditional harmonic estimation methods, by utilizing Artificial Intelligence, these requirements are minimized. In this paper, a comprehensive review of traditional and modern (smart) harmonic estimation techniques are discussed.

INDEX TERMS Power quality, harmonic distortion, artificial intelligence, machine learning, neural network, power systems, harmonic estimation, harmonic mitigation.

I. INTRODUCTION

Power electronic converter-fed devices and equipment such as computers, Adjustable Speed Drives (ASDs), and Light-Emitting Diodes (LEDs) for lighting are frequently used in industrial applications and distribution networks. Therefore, due to a massive employment of such devices and their non-linear behavior in power systems, power quality has emerged as a major concern for energy companies and network operators [1], [2]. The efficiency of electrical equipment is affected by a range of power quality issues, including voltage and current harmonics, interharmonics, voltage instability (sag and swell), flicker, voltage notch, transient instability, and grid imbalance [3]. Among them, harmonic distortion is the most significant factor which manifests as voltage and current emissions. Harmonics will heat up motors, cables, and transformers, reduce efficiency, nuisance in operating circuit breakers, and create notch voltages, lightning strikes, grid

The associate editor coordinating the review of this manuscript and approving it for publication was Frederico Guimarães.

instability and network equipment misoperation. It is worth noting that nonlinear loads alter the sinusoidal nature of the AC supply current, causing harmonic currents to flow through the AC power system and potentially disrupting communication circuits and other types of devices. Additionally, these harmonic currents increase heating and losses in a variety of electromagnetic equipment (motors, transformers, etc.) [4]. Resonant circumstances that can lead to large levels of harmonic voltage and current distortion can arise when reactive power compensation, in the form of power factor improvement capacitors, is utilized. This is especially true when the resonance condition occurs at a harmonic due to nonlinear loads [5]. The main contributors of harmonics in power systems are power electronic switching devices and converters acting as non-linear loads, ASDs, Electric Vehicle (EV) chargers, LED fluorescent lights, and computer power supplies.

In a variety of industrial applications, circuit configurations such as motor drive systems with a diode-rectifier front-end and a rear-end inverter are increasingly employed. It is estimated that the consumption of Motor Drive systems accounts for 46% of all worldwide electricity, which makes the manufacturers improve the network's power quality, efficiency, and energy management [6]. An ASD at a unit/product level with a distribution network connected to the three-phase diode-rectifier and DC-choke filter is presented in Fig. 1. In this circuit, Z_g is the grid impedance, and the DC-choke impedance is formed by L_{dc} and R_{dc}, and the DC-link capacitor's impedance is represented by C_{dc} and R_c. It is worth mentioning that single-phase and three-phase power electronic equipment are the sources of current harmonics, which in combination with grid impedance results in voltage harmonics.

Fig. 2 shows the rectified voltage across the DC-link, and input phase "a" voltage of a 7.5 kW ASD system. Additionally, it shows how the switching function of the diode-rectifier influences the rectified current and generates the input currents that the ASD system uses (e.g., i_a). It is found that the three-phase diode-rectifier is the primary contributor to current harmonics for the frequency range of 0–9 kHz [7]. Additionally, the operational power of other drive systems in the network has an impact on the amplitude of these current harmonics. Switching function of phase "a" (Sa) can be defined to determine the current harmonics produced by the diode rectifier, as below:

$$S_a = \frac{4}{\pi}\sum_{k=0}^{+\infty}\frac{\cos\frac{(6k+1)\pi}{6}}{6k+1}\sin\left((6k+1)\,\omega t+\theta_{Sa,6k+1}\right) + \frac{4}{\pi}\sum_{k=0}^{+\infty}\frac{\cos\frac{(6k-1)\pi}{6}}{6k-1}\sin\left((6k-1)\,\omega t+\theta_{Sa,6k-1}\right) \tag{1}$$

where $\theta_{sa,6k\pm1}$ stands for a harmonic phase angle with orders of $6k \pm 1$. The grid current i_a is then derived by $S_a \times i_{rec}$. This equation demonstrates that the rectifier produces the harmonics $I_{a,h}$ at $h = (6k\pm1)$. It is also revealed that the 2–9 kHz current harmonics created by rear-end inverter are damped through a large capacitor at the DC-link that also has a diode-rectifier and a DC-choke filter connected.

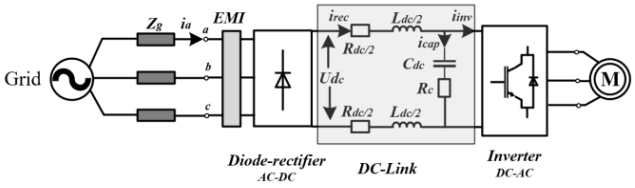

FIGURE 1. Typical ASD with three-phase diode-rectifier.

In a multi-parallel system, several parallel connected converters with numerous sources of power (e.g., solar farms) are utilized at PCC to increase the quantity of injecting current in the network. The harmonics generated by power electronic converters at the system level can deteriorate the power quality across the distribution network, due to harmonic interaction, resonance, and grid impedance (transformer and distribution cables) and finally lead to increase losses in the network. The power quality at the PCC is very important because it can affect the other connected equipment.

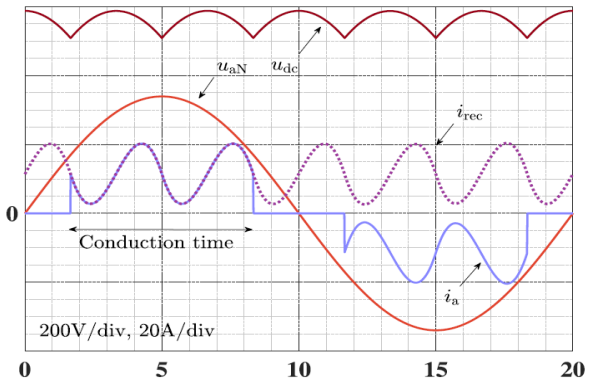

FIGURE 2. Input voltage, current, and the rectified voltage and current of a typical ASD at a stiff grid [7].

In contrast to a single grid-connected inverter, each inverter in a multi-drive system utilizes a varied harmonic rejection capability and consumes output current from other inverters depending on its own impedance. Therefore, analyzing the interaction between the inverters in multi-parallel grid-connected equipment is the main challenge. Fig. 3 shows a multi-parallel drive system. In a parallel set of inverters, the output current of each inverter is susceptible to harmonics from three separate sources. First, the reference signal source of the inverter has the possibility to distort the grid side ccurrent of the inverter. If high-level harmonics are introduced into the inverter through the Phase Locked Loop (PLL), the reference signal source may contain harmonics other than the fundamental component. Secondly, other inverters' reference signal sources may also become distorted, however, they will have different impacts on the grid side current of the inverter.

As a result, the reference signal sources of other inverters serve as the second type of harmonic source for an inverter connected in parallel. The third source of harmonic is the grid voltage which causes current harmonics on the grid-side inverter.

In order to minimize the presence of harmonics in power systems, mitigation techniques have been proposed in a wide range of strategies. It has been demonstrated that a harmonic mitigation capability depends on a variety of factors, including grid inductance, characteristics of the transformer, structure of the system, load profiles, and topologies [8], [9]. Devices such as Unified power quality conditioners (UPQC) [10], passive damping filters [11], Active Power Filters (APF) [12], Electronic Inductors (EI) [13], D-STATCOMs [14], and techniques such as selective harmonics compensation [15], Finite, and Infinite Impulse Response (FIR) and (IIR) filters [16], are among the most popular mitigation devices and techniques which have been used to suppress harmonic emissions in distribution networks. While it is essential to use effective strategies to reduce or eliminate harmonic distortions in power systems, it is more crucial to estimate these harmonics at the outset by coming up with smart, effective, and precise techniques. Harmonic estimation entails determining the properties of harmonic emissions in a distorted signal [17], [18], which is necessary in power systems to mitigate harmonics and consequently ensure the required power quality standards are met. These properties include the phase and amplitude of each harmonic component in a measured signal. There are many techniques for estimating the harmonics in distribution networks, such as Bayesian [19], Fast Fourier transform (FFT) [20], Harmonic State Estimation (HSE) [21], Particle Swarm Optimization (PSO) [22], etc. Recently, many converters are employed in power systems in which their cumulative contribution to harmonics goes beyond simple addition.

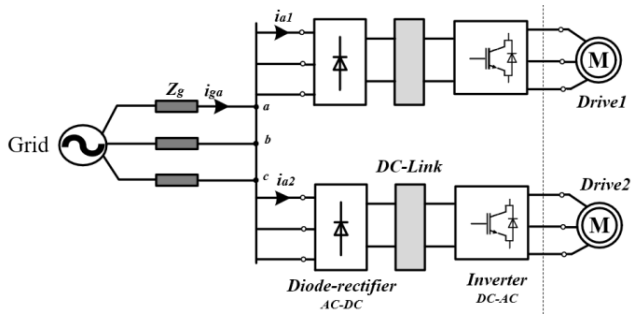

FIGURE 3. Multi-drive network with parallel connected ASDs.

As a result, the traditional analytical techniques employed to determine and accurately measure the real quantity of harmonics are ineffective. Statistical techniques such as the Unscented Transform (UT), Monte Carlo Simulation (MCS), and others may be used to solve this difficulty, but their computing costs and time requirements are quite high [23], [24].

Artificial intelligence (AI) describes a computer's capacity to imitate human cognitive learning and comprehension. In recent decades, it has drawn a lot of interest for its use in several branches of science. In the operation, control, and monitoring of electricity networks, a vast amount of data is collected and used. Signal processing, prediction, and control are just a few applications where artificial intelligence systems have performed well. Therefore, utilizing AI, Machine Learning (ML), neural networks (NN), Fuzzy Logic (FL), and Genetic Algorithm (GA) are other options for smart harmonics estimation with manageable processing demands and time.

In this paper, a comprehensive review of power quality issues- in specific, harmonic distortion- in power systems has been presented. Different mitigation techniques are investigated, and conventional harmonic estimation methods are studied. To cope with the issues associated with the conventional estimation methods, new smart AI approaches have been reviewed as an alternative which are fast, accurate and efficient. Due to their capabilities in learning, predicting, and identifying, researchers tend to use these AI-based techniques more frequently.

II. HARMONIC STANDARDS

To investigate harmonic emissions in power systems, international standardization groups e.g., the IEC and IEEE have developed many power quality standards. The related standards are created to limit harmonic emission at the product and the system level, according to test conditions, such as establishing the grid voltage with or without any background harmonic. Harmonic limits are used in power systems to restrict the harmonic injection from individual customers to the grid so that it does not result in excessive grid voltage distortion. The existing IEC or IEEE standards are defined to cover the harmonics limits for different frequency ranges which are described as follows.

A. DIFFERENT FREQUENCY RANGES

A resonant frequency can be produced in a power electronic converter with a DC-link capacitor with a line impedance below and over 1kHz [25]. Numerous variables, including load power levels, filter types, and the number of parallel drives, influence the resonance effects. These problems can have an impact on the power quality of the distribution networks and harmonic emissions of the grid current. As seen in Fig. 4, there are no standard guidelines or compatibility levels for harmonics in the 2-150 kHz range to protect all electrical networks and grid-connected devices. Therefore, future grids will face new difficulties related to these new frequency ranges, which can be categorized as follows: 1) the production of high-frequency harmonics, 2) the development of new resonance frequencies, and 3) the strength of harmonic interactions between various power electronic system types.

A significant portion of the inverter current harmonics between 2-150 kHz can transfer to the grid-side inverter current in a power converter with a diode rectifier and

motor-side inverter. Because of the series connection of inductive and resistive components having a larger impedance in the 2-150 kHz frequency range, in a realistic non-ideal DC-link capacitor of the drive system, the high-frequency inverter input current harmonics cannot be properly absorbed. Consequently, it is crucial to have a mathematical knowledge of the motor-side inverter input current harmonics in order to examine the grid-side current harmonics based on the DC-link capacitor and grid impedance characteristics. According to Fig. 4, the current technical standards, which are based on IEC 61000-3-2, IEC 61000-3-12, IEEE 519, and the International Special Committee on Radio Interference, respectively, cover all grid-connected systems for frequency ranges between 0 and 2 kHz and above 150 kHz. However, the most crucial issues in the international standardization committee, immunity, and emission limits, and measurement methods such as at product and system levels for harmonics within the frequency ranges of 2-9 and 9-150 kHz, are currently lacking (IEC, TC77A).

To deal with this issue, international experts have been asked by the IEC Technical Committee 77A (TC 77A), to provide practical records for international standards, and to define standardization for harmonics within the frequency range of 2-150 kHz [26]. The definition of compatibility levels for the frequency ranges of 2-9 and 9-150 kHz has been developed for residential network and under development for industrial networks in IEC-TC77A-WG8 [27], [28].

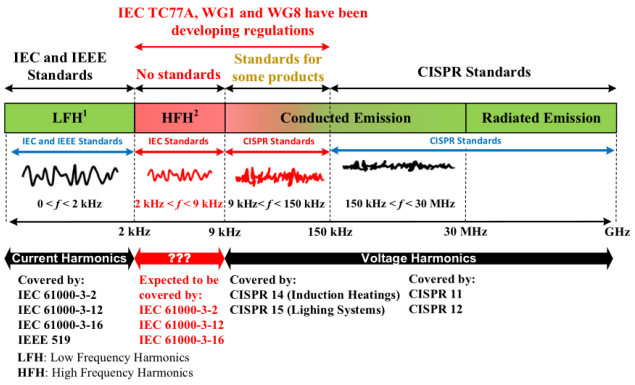

FIGURE 4. Different frequency ranges of harmonics emission categorized by IEC for distribution networks [27].

Emission and immunity levels at the product level will be defined in the future. The most important standards for harmonic limits are IEEE 519, IEC 61000-3-2, and IEC 61000-3-12 which are described as follows.

B. IEEE 519 STANDARD

The limits outlined in IEEE 519 standard signify a common obligation for harmonic emissions between system owners, operators, and users. Users generate harmonic currents that pass through the infrastructure of the system operator or owner, which results in voltage harmonics delivered to other users. The total impacts of the harmonic current producing loads of all users and the impedance properties of the supply system determine how much harmonic voltage distortion is supplied to other users. To minimise the potential risk to end users and system equipment, harmonic voltage distortion restrictions are offered. The limits in IEEE 519 standard are meant to be applied at a point of common coupling (PCC) between the vendor or operator of the system and a customer. The PCC is typically understood to be the location in the power system closest to the customer at which the vendor or operator of the system could provide service to another customer. Voltage harmonics whose frequencies are integer multiples of the power frequency are presented in Table 1. The users' current value is determined by the PCC and is calculated by dividing the total currents that correspond to the maximum demand during each of the 12 months divided by 12. For harmonic currents with integer multiples of the power frequency, Table 2 is applicable [29].

TABLE 1. Voltage distortion limits.

Bus voltage V at PCC	Individual harmonic (%)	THD (%)
$V \leq 1.0\ KV$	5.0	8.0
$1.0\ KV < V \leq 69\ KV$	3.0	5.0
$69\ KV \leq V \leq 161\ KV$	1.5	2.5
$161\ KV < V$	1.0	1.5

TABLE 2. Current distortion limits.

Maximum harmonic current distortion in percent of I_L						
Individual harmonic order (odd harmonics)						
I_{SC}/I_L	3≤h<11	11≤h<17	17≤h<23	23≤h<35	35≤h<50	TDD
<20	4.0	2.0	1.5	0.6	0.3	5.0
20<50	7.0	3.5	2.5	1.0	0.5	8.0
50<100	10.0	4.5	4.0	1.5	0.7	12.0
100<1000	12.0	5.5	5.0	2.0	1.0	15.0
>1000	15.0	7.0	6.0	2.5	1.4	20.0

C. IEC 61000-3-2 STANDARD

IEC 61000-3-2 is an international standard called limits for harmonic current emissions for equipment with voltage greater than 220 volts and current up to 16 A per phase, setting the upper limit for harmonic currents from the 2nd harmonic up to and including the 40th harmonic current to reduce mains voltage distortion. An important issue with pollution by current harmonics has emerged with the introduction of large-scale distributed electronic equipment, first the radio with electronic valves, then TV, and finally personal computers.

This current flows through such equipment show input current shape in the peaks and valleys of the AC wave because of having rectifiers linked with large value smoothing capacitors. It is worth noting that the current flows through the massive smoothing capacitors for a short period (Fig. 5); therefore, the half-cycle current waveform lasts for 10 *ms* as an example. As a result, a large peak current flow occurs within a short period. Such pure and smooth equipment can have a power factor as low as 0.6 and generate a significant number of harmonics (shown in Table 3).

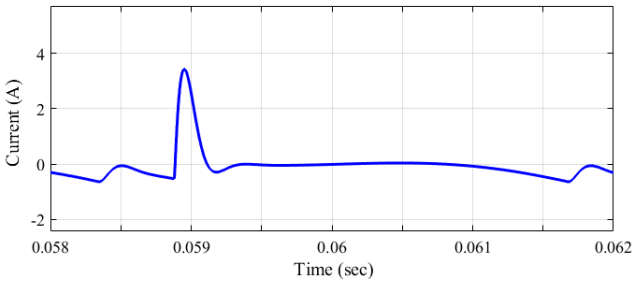

FIGURE 5. Short period spike current of a DC-link capacitor.

TABLE 3. The emissions limits in IEC 61000-3-2.

Harmonic order 'n'	Max current Class A	Max current Class B	Max current Class C (% of fundamental current)	Max current Class D (but no more than class A)
2	1.08 Amps	1.62 A	2 %	not specified
3	2.3 A	3.35 A	30 λ %	3.4 mA/Watt
4	0.43 A	0.645 A	not specified	not specified
5	1.14 A	1.71 A	10 %	1.9 mA/Watt
6	0.3 A	0.45 A	not specified	not specified
7	0.77 A	1.155 A	7 %	1.0 mA/Watt
8≤n≤40 (even)	0.23 (8/n) A	0.345 (8/n) A	not specified	not specified
9	0.4 A	0.6 A	5 %	0.5 mA/Watt
11	0.33 A	0.495 A	3 %	not specified
13	0.21 A	0.315 A	3 %	0.35 mA/Watt
15≤n≤39 (odd)	0.15 (15/n) A	0.225 (15/n) A	3 %	(3.85/n) mA/Watt

D. IEC 61000-3-12 STANDARD

IEC 61000-3-12 establishes limitations for harmonic current values in systems rated from 16 A to 75A per phase and the nominal voltage up to 230/400 V for single-phase/three-phase. If we consider R_{sce} as a short circuit ratio, the minimum requirement is R_{sce} =33 and above for most commercial equipment. It is worth mentioning that higher emission values can be considered for equipment (with the input current above 16 A per phase) not fulfilling the harmonic current emission limits defined for the specific R_{sce} in the standard. Table 4 is applied to equipment other than balanced three-phase equipment and tables 5, 6 and 7 are applied to balanced three-phase equipment. Table 5 might be used for any balanced three-phase piece of equipment. Table 6 can be used with balanced equipment if: a) the phase angle of the 5th harmonic current related to the fundamental phase-to-neutral voltage is in the range of 90^{o} to 150^{o} (uncontrolled diode-rectifier with smoothing capacitor), b) the equipment is designed in a way that the phase angle of the 5th current harmonic has no preferential value over time and can take any value between 0 and 360° (controlled bridge converters), and c) either 5th and 7th current harmonics are below the 5% of the fundamental reference current.

TABLE 4. Current emission limits for equipment other than balanced three-phase equipmen.

Min Rsce	I_3	I_5	I_7	I_9	I_{11}	I_{13}	THC/I_{ref}	$PWHC/I_{ref}$
33	21.6	10.7	7.2	3.8	3.1	2	23	23
66	24	13	8	5	4	3	26	26
120	27	15	10	6	5	4	30	30
250	35	20	13	9	8	6	40	40
≥350	41	24	15	12	10	8	47	47

TABLE 5. Current emission limits for balanced three-phase equipment.

Min Rsce	I_5	I_7	I_{11}	I_{13}	THC/I_{ref}	$PWHC/I_{ref}$
33	10.7	7.2	3.1	2	13	22
66	14	9	5	3	16	25
120	19	12	7	4	22	28
250	31	20	12	7	37	38
≥350	40	25	15	10	48	46

TABLE 6. Current emission limits for balanced three-phase equipment under specified conditions (a, b & c).

Min Rsce	I_5	I_7	I_{11}	I_{12}	I_{13}	THC/I_{ref}	$PWHC/I_{ref}$
33	10.7	7.2	3.1	1.3	2	13	22
≥ 120	40	25	15	1.3	10	48	46

TABLE 7. Current emission limits for balanced three-phase equipment under specified conditions (d, e & f).

Min Rsce	I_5	I_7	I_{11}	I_{13}	I_{17}	I_{19}	I_{23}	I_{25}	I_{29}	I_{31}	I_{35}	I_{37}	THC/I_{ref}	$PWHC/I_{ref}$
33	10.7	7.2	3.1	2	2	1.5	1.5	1.5	1	1	1	1	13	22
≥250	25	17.3	12.1	10.7	8.4	7.8	6.8	6.5	5.4	5.2	4.9	4.7	35	70

Table 7 can be used with balanced equipment if any of these conditions is met: d) the phase angle of the 5th harmonic current related to the fundamental phase-to-neutral voltage is in the range of 150^{o} to 210^{o} (6 pulse converter with a small DC link capacitance, operating as a load), e) the equipment is designed in a way that the phase angle of the 5th current harmonic has no preferential value over time and can take any value between 0 and 360° (controlled bridge converters), and f) either 5th and 7th current harmonics are below the 3% of the fundamental reference current.

The existing IEC standards IEC61000-3-2 and IEC61000-3-12 cannot be used for the frequency range of 2-9 kHz. For a grid with a fundamental frequency of 50 Hz, these regulations only offer emission limitations for frequencies up to 2 kHz. Similarly, the other well-known standard IEEE 519-2014, which only covers up to 2.5 kHz, is ineffective for 2-9 kHz harmonics. Additionally, rather than focusing on the current harmonics produced by a single device, IEEE 519-2014 aims to keep the overall harmonic distortions at the PCC below a certain threshold.

III. HARMONIC MITIGATION TECHNIQUES

Harmonic mitigation, which involves taking actions to reduce harmonics in power system networks, can result in

increasing the efficiency, increasing the lifespan of equipment, and improving the performance of the systems. The harmonic mitigation techniques can be classified based on the unit level and system level which are described as follows.

A. HARMONIC MITIGATION TECHNIQUES AT UNIT LEVEL

Active and passive filters are harmonic mitigation techniques which are developed significantly, mainly focusing on the line harmonic control at the distribution network. Passive and active filters also utilize to fulfill the current harmonic requirements defined in relevant standards. Fig. 6 shows a motor drive at the unit level with different DC-side passive filters (e.g., DC choke or AC choke, small DC-link capacitor, as well as tuned filters). Fig. 7 also shows time & frequency domain waveforms to show a comparison of DC choke and Slim DC for the frequency ranges of below 2 kHz and 2-9 kHz.

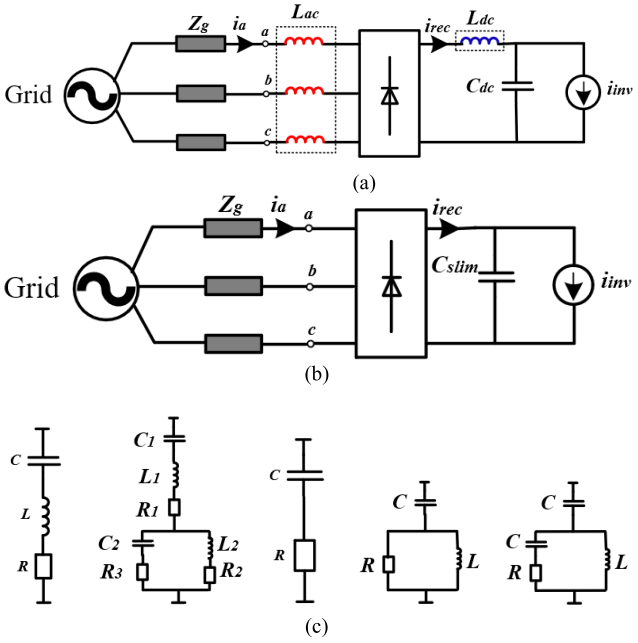

FIGURE 6. A motor drive system at unit level with (a) AC-choke and DC-choke (b) small capacitor filters (c) passive-tuned filters.

Fig. 8 depicts a single-phase grid-connected inverter with a passive damping LCL filter. This structure consists of an inverter, an AC side filter, a control loop, and a DC supply/load, connected with a DC-link capacitor [30]. In this system, PWM methods are used for switching the power inverter switches. Grid-tied inverter output current is subject to high-frequency ripples and harmonics because of this PWM. A variety of filters may be applied to the inverter output terminals to reduce these ripples and harmonics. However, compared to L-filters, LCL filters are more efficient in reducing high-frequency ripples and harmonics. To reduce the effect of grid voltage distortion on the injected current, a novel full-feedforward approach is presented in [31].

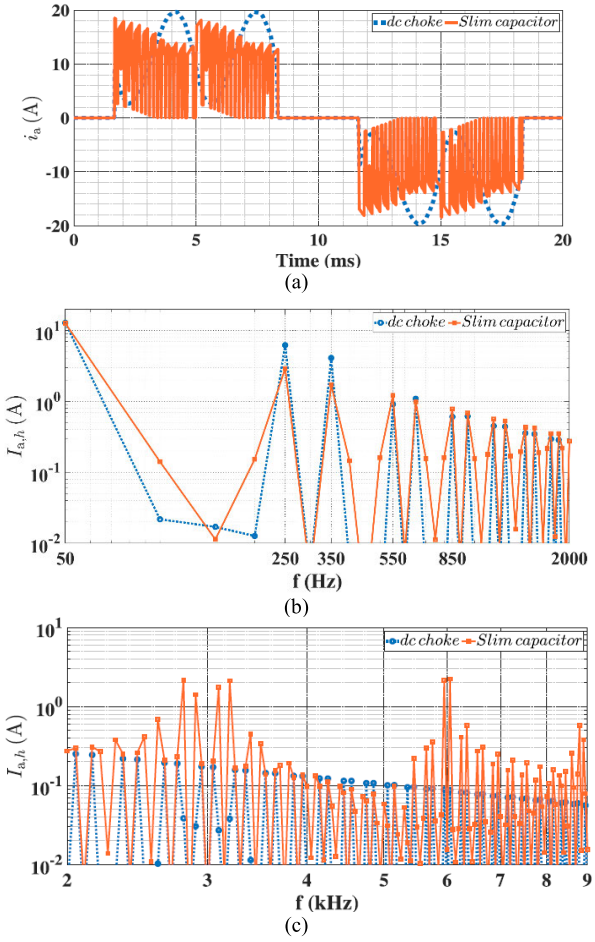

FIGURE 7. Time and frequency domain current waveform DC choke and slim capacitor comparison (a) Time domain current waveform (b) frequency domain waveform for below 2kHz, and (c) frequency domain waveform for 2-9kHz range [7].

In this method, the transfer function of feedforward control has been employed in only one of the inverters (target inverter). There has also been proposed a complementary selection approach that ensures the desired harmonic cancellation capacity against dominating grid voltage harmonics. In fact, the main aim of the proposed control is to inject a high-quality current into the network. As a result, the grid current includes the minimum harmonic levels regardless of the grid voltage background harmonics. The feedforward

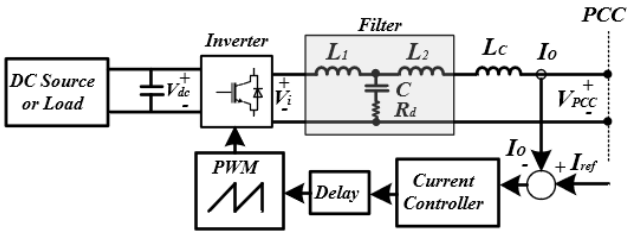

FIGURE 8. A grid-connected inverter with passive damping LCL filter.

transfer function greatly reduces the low-order grid current harmonics. However, because the phase margin requirements were lowered in this instance, the operation mode was found to be unstable. Due to system instability, high frequency grid voltage harmonics significantly distort the grid current.

Active Front End (AFE) configuration also can mitigate the low-frequency harmonics (below 2kHz) at the unit. Fig. 9 shows an AFE with an LCL filter proposed in [32]. Fig. 10 (a) corresponds to the experimental results of the time domain grid current waveform of a damped AFE proposed in [32]. Fig. 10 (b) and (c) also depict the frequency domain waveform (FFT analysis) of the mentioned current for the ranges of 0-2 kHz and 2-9kHz. It is worth noting that the grid current THD for the range of 0-2 kHz is measured at 2.78 % for 1 cycle or 2.95 % for 10 cycles.

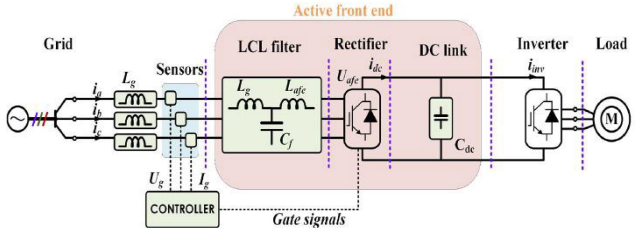

FIGURE 9. Configuration of AFE proposed in [32].

By connecting a simple resistor to the filter, a passive damping technique can successfully minimize the resonance peak. The resonance peak decreases with increasing resistor size. A unified process for designing an LCL filter for a grid-connected inverter is proposed in [30]. In this research, for calculating the inverter's maximum current ripple, mathematical calculations are used. Another LCL filter with passive damping resistors designed for grid-connected inverters has been proposed in [33] to handle injected harmonics to the grid. The main contribution of this research is to increase the robustness and stability of the grid-connected inverter by proposing a mathematical approach to calculate the maximum current ripple as well as the inductor size on the inverter-side.

International standards permit three-phase diode rectifier systems to generate a relatively high degree of current total harmonic distortion (THD_i). As an instance, according to IEC61000-3-12, for a system with a current of 16–75 A per phase, the THD_i is allowed to be up to 48% (5^{th} harmonic allowed to be 40%) [34]. However, the dependence of THD_i on the load level is the primary disadvantage of the traditional diode rectifiers with a passive filter (DC or AC choke). As a result, the THD_i can significantly rise during partial-power operation which ASDs normally follow most of the time. To cope with these challenges, Electronic Inductor (EI) (a DC-DC boost converter) cascaded to the diode-rectifier, can be used as an alternative to the passive filters as illustrated in Fig. 11. The EI positioned at the DC-link stage can emulate an active-front end in addition to the diode rectifier. The fundamental concept behind employing EI is to substitute

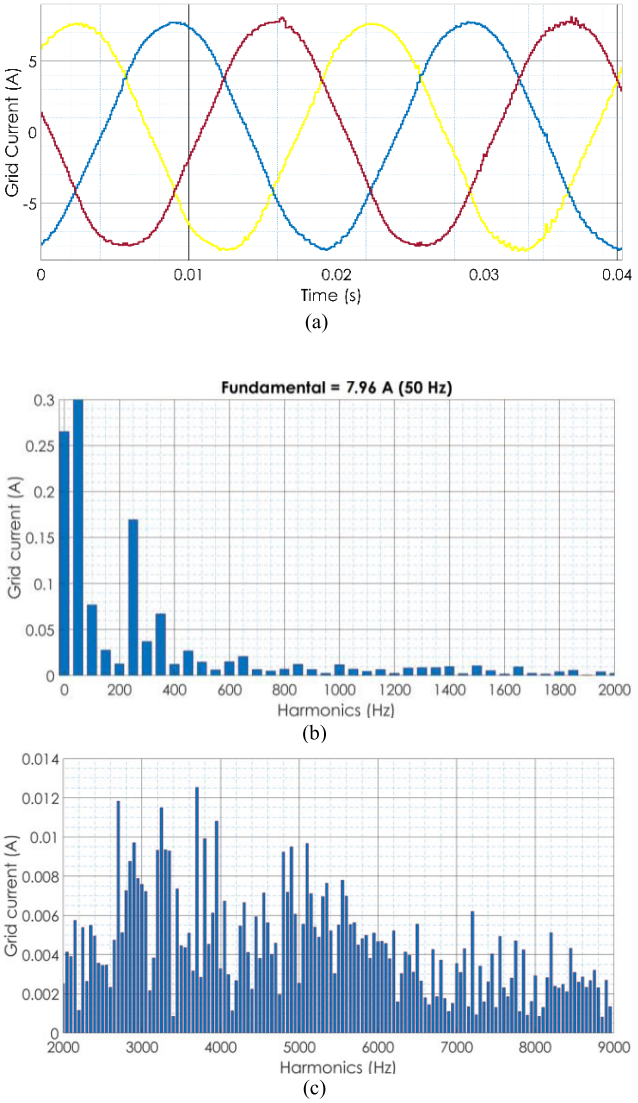

FIGURE 10. Time and frequency domain waveform of the AFE proposed in [32] (a) Current waveform of damped AFE (b) 0-2kHz (c) 2-9kHz.

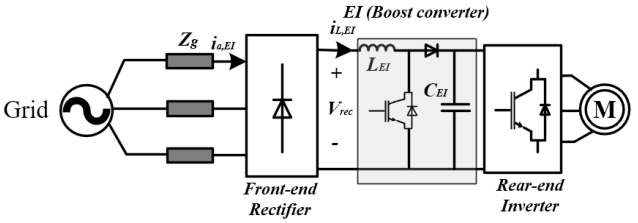

FIGURE 11. An ASD at unit level with front-end diode-rectifier and EI filter.

the large DC choke with a smaller inductor that relates to a DC-DC converter to operate like an ideal infinite inductor, which can greatly enhance the quality of the drive's current.

B. HARMONIC MITIGATION TECHNIQUES AT SYSTEM LEVEL

Typically, it is believed that a power converter's harmonic performance is the same at the unit and system levels. As a result,

by implementing harmonic mitigation strategies at the unit level, it is anticipated that the existing harmonic issues will be predicted and resolved at the system level. However, due to variations in phase angle, current harmonics for parallel converter units may be canceled at the system level [25].

The unified power quality conditioner (UPQC), also referred to as the universal active filter, which consists of both series and shunt active power filters (APFs), is the most comprehensive configuration of hybrid filters as shown in Fig. 12 [35]. UPQC is a multipurpose power conditioner that can be used to correct voltage fluctuations, compensate for different power source voltage disturbances, and block harmonic load current from entering the power system. It is a special power tool made to lessen disturbances that interfere with the execution of sensitive and/or important loads. A UPQC is typically made up of a shunt inverter, which by injecting shunt current can control the reactive power and reduce harmonic emissions, and a series inverter, which can reduce the voltage sag/swell issues.

In the simplest form, the shunt APF, also known as D-STATCOM structure includes a two-level VSC, a DC energy storage system, a shunt coupling transformer, and related control equipment. Fig. 13 shows a schematic representation of a D-STATCOM as a custom power controller. The VSC attached in shunt to the AC system can give a multipurpose topology which can be utilized for up to three very different objectives, including voltage control and compensation of reactive power, power factor correction, and current harmonic mitigation [36]. It is worth noting that in PV applications, the seasonal and daily solar radiation variations have

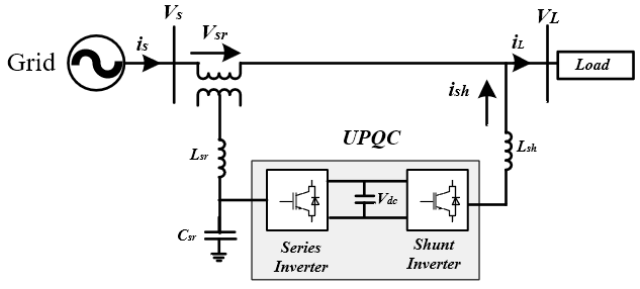

FIGURE 12. General configuration of a UPQC.

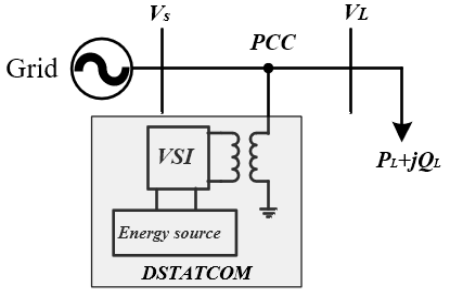

FIGURE 13. Schematic diagram of D-STATCOM as a custom power controller.

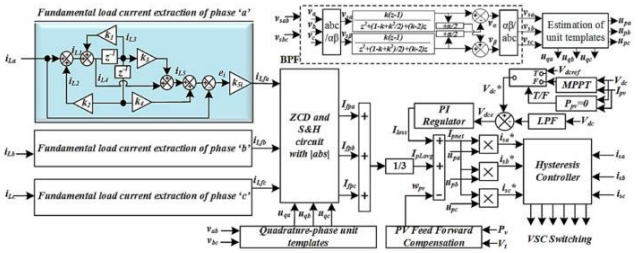

FIGURE 14. Control technique based on IIR peak filter proposed in [16].

an impact on the electricity generated by a solar PV array. Additionally, the utility distribution networks are generally weak, which worsens problems with power quality degradation. The development of an infinite impulse response (IIR) peak filter is required for harmonics mitigation, power factor correction, and alleviating other power quality concerns by offering D-STATCOM capabilities. In order to ensure effective operation under weak grid situations, a novel control strategy using an IIR peak filter for grid-fed PV generation in the distribution network is proposed in [16], as shown in Fig. 14. This control method is effective when solar PV power cannot be obtained. The solar PV array and the grid power that has been saved are used to meet the load requirements during the day. On the other hand, DSTATCOM performance ensures an improvement in power quality at night when the solar PV array's output is not available to meet the load requirements.

A novel technique using Harmonic Mitigation Function (HMF) based on EI circuit is proposed in [37] which can mitigate harmonics generated by other commercial and industrial motor drives. This technique can reduce the current harmonics produced by other units with passive filters, which are connected to the same PCC. The phase-angle of low-order harmonics are also stabilized and meet the IEC 61000-3-12 requirements. As a result, a distribution network with several drive units can also eliminate harmonics using the proposed converter and control system. The diagram of proposed EI-based technique including both a square wave and a ripple component, is shown in Fig. 15 (a). Fig. 15 (b) depicts the system with two units, where Unit 1 is an EI-based converter as the intermediate circuit (DC choke) and Unit 2 is a traditional converter with a passive filter. As a result, the EI controller is altered to maintain the appropriate output voltage and simulate an AC ripple with a 180-degree phase shift that is the same magnitude as the AC ripple of the conventional unit. Therefore, the AC ripples cancel out each other at the PCC, resulting in a square-shape total input current (i_{ga}) with a load-independent THD_i of around 30%.

The ability of the current control system to closely follow the reference current and quickly inject the necessary currents into the grid to reduce harmonics is critical to the operation of the Active Power Filter (APF). However, from the operating environment point of view, there are external disturbances brought on by the load and source sides, as well as internal perturbations caused by component aging and thermal

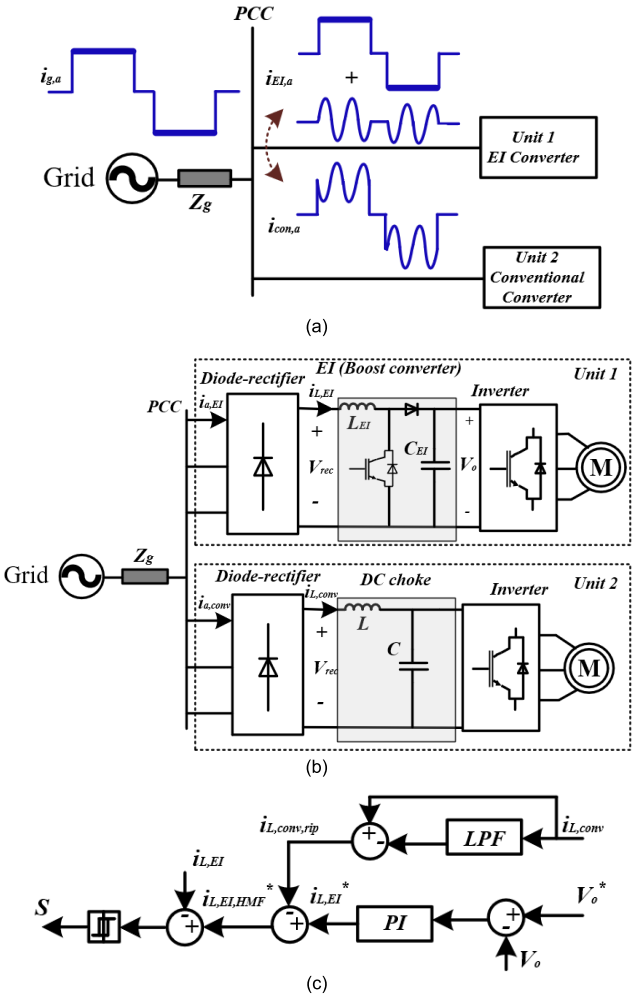

FIGURE 15. The technique proposed in [37]. (a) the current component of the units (b) an EI connected to unit 1 and unit 2 equipped with a passive filter (c) the proposed control strategy.

drift. Utilizing a robust control method is crucial because it offers adequate disturbance rejection against uncertainties. Generally, sliding mode control (SMC) is a common strong design for uncertainties. Additionally, considering real applications, the development of terminal sliding mode control (TSMC) gives classical SMC finite-time convergence properties, which is desirable for APFs. However, the issue is that the TSMC is dependent on the prior information. Fuzzy and neural network techniques can be employed as universal approximators to cope with these challenges. An adaptive type-2 fuzzy neural network (T2FNN) inheriting TSMC to improve the power quality of the system is proposed in [38]. Then, a finite-time reference signal tracking integral-type TSMC is created which uses a saturation function to address the chattering problem. This paper suggests a method for controlling APF that not only completes the required harmonic suppression duty but also offers robustness and releases some constraints. It is worth mentioning that to suppress harmonics, it is important to propose a controller which can reduce the tracking error between the compensation and reference signals of the current. Fig. 16 illustrates the proposed T2RFSFNN control diagram. If the dynamic model of APF current control is extracted from the following equation:

$$\dot{i}_c = f\,(i_c) + U + H \tag{2}$$

And the control of T2RFSFNN law is designed as follows:

$$U = U_{T2RFSFNN} + U_{COM} \tag{3}$$

The proposed control algorithm [38] can be obtained as:

$$\dot{\hat{W}}_H^T = -\dot{\tilde{W}}_H^T = -\lambda_1 \hat{\eta} s \hat{Y}_H \tag{4}$$

$$\dot{\hat{W}}_H^T = -\dot{\tilde{W}}_L^T = -\lambda_2 (1-\hat{\eta}) s \hat{Y}_L \tag{5}$$

$$\dot{\hat{\mu}}^T = -\dot{\tilde{\mu}}^T = -\lambda_3 [\hat{\eta} s \hat{W}_H Y_{H\mu} - (1-\hat{\eta})\, s \hat{W}_L Y_{L\mu}] \tag{6}$$

$$\dot{\hat{\bar{\sigma}}}^T = -\dot{\tilde{\bar{\sigma}}}^T = -\lambda_4 \hat{\eta} s \hat{W}_H Y_{H\bar{\sigma}} \tag{7}$$

$$\dot{\hat{\underline{\sigma}}}^T = -\dot{\tilde{\underline{\sigma}}}^T = -\lambda_5 (1-\hat{\eta}) s \hat{W}_L Y_{L\bar{\sigma}} \tag{8}$$

$$\dot{\hat{\omega}}_r^T = \dot{\tilde{\omega}}_r^T = -\lambda_6 [\hat{\eta} s \hat{W}_H Y_{H\omega_r} - (1-\hat{\eta})\, s \hat{W}_L Y_{L\omega_r}] \tag{9}$$

$$\dot{\hat{\bar{\beta}}}^T = -\dot{\tilde{\bar{\beta}}}^T = -\lambda_7 \hat{\eta} s \hat{W}_H Y_{H\beta} \tag{10}$$

$$\dot{\hat{\underline{\beta}}}^T = -\dot{\tilde{\underline{\beta}}}^T = -\lambda_8 (1-\hat{\eta}) s \hat{W}_L Y_{L\underline{\beta}} \tag{11}$$

$$\dot{\hat{\eta}} = -\dot{\tilde{\eta}} = -\lambda_9 s (\hat{W}_H \hat{Y}_H - \hat{W}_L \hat{Y}_L) \tag{12}$$

$$U_{COM} = -\hat{k} sat(\frac{s}{\eta}) \tag{13}$$

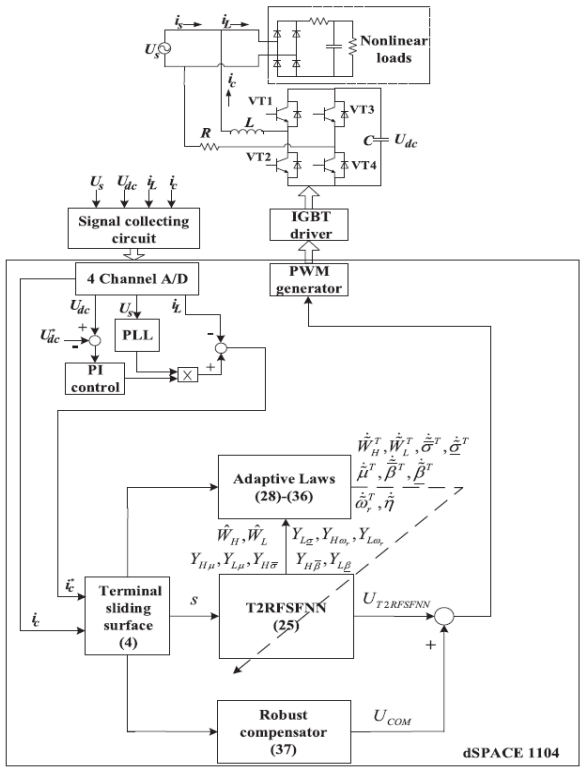

FIGURE 16. Block diagram of T2RFSFNN control methodology for APF [38].

And the robust compensator can be designed as follows:

$$\dot{\hat{k}} = -\dot{\tilde{k}} = \lambda_{10}\,|s| \tag{14}$$

IV. TRADITIONAL HARMONIC ESTIMATION TECHNIQUES

Harmonics are one of the main causes of the power system's deteriorating power quality. Therefore, it is essential to estimate the amplitude and phase angle of the injected harmonics in a power system network. In this section, a critical analysis of numerous power system harmonic estimation techniques is presented. Regulators are now focused on ensuring that distributors fulfill their responsibilities of maintaining power quality. Even though most distribution network service providers (DNSPs) now consider collecting power quality data to be a routine aspect of conducting business and that substantial amounts of data are routinely recorded and stored, there are still considerable difficulties associated with power quality monitoring. These difficulties include developing efficient power quality monitoring plans, such as the optimal number of instruments and deployment locations, managing power quality parameters, and comprehending the financial effects of power quality on customers and networks.

Generally, there are two types of harmonic estimation techniques, which are parametric and non-parametric methods. In parametric methods, a proper model can be used to represent the voltage and current signals and then estimate the parameters from the data. On the other hand, non-parametric methods can estimate the spectrum directly from the voltage and current signals in terms of amplitude and phase angles, etc.

A. PARAMETRIC HARMONIC ESTIMATION METHODS

An analytical method for estimating the current harmonics of an ASD on the DC-link at the inverter side is proposed in [39]. In this paper, the impacts of unbalanced loads and power factors on the current harmonics for the frequency range between 0-9 kHz have been analyzed. Moreover, new mathematical modeling has been developed for current harmonic orders which are impacted by negative-sequence current. Another contribution of this paper is identifying 2–9 kHz current harmonics produced by ASD due to PWM modulation. These current harmonics are among the important topics under consideration for IEC standardization SC77A. The effects of positive and negative sequence currents on the inverter-side current harmonics in a frequency range of 2–9 kHz is also estimated. This can make it simpler for drive manufacturing businesses to determine the current harmonics over the ASD DC bus while considering the unbalanced-load condition.

As mentioned before, the harmonics over 2 kHz have been considered in recent years by several standardization committees to prevent EMI issues in electronic equipment. As a result, network operators need to estimate harmonics in networks to maintain the required power quality at the PCC. To achieve this goal, manufacturers seek accurate models to assess ASD harmonics in accordance with current and future standards. The study in [40] presents the development of a novel mathematical model for the estimation of the inverter-side current harmonics flowing across the DC-link in an ASD considering the voltage harmonic impacts. When determining the current harmonics at the load side of the ASD, this model is implemented by considering an accurate model of voltage ripples over the DC-link. Additionally, the grid-side current harmonics may be estimated for filter design applications using the estimated inverter-side current harmonics. It is important to note that depending on the harmonic components, the frequency of the inverter-side current harmonics can be split into several categories. One of them includes portions relating to the fundamental frequency of the load side voltage, the switching frequency of the rear-end inverter, and the harmonics of the DC-link voltage, whereas the other category just includes the harmonics of the ripples in the DC-link voltage.

Although the harmonics generated by a single household device are insignificant, but recent research has shown that the combined effect of large domestic loads can be considerable. Telephone interference, pipeline corrosion, utility asset overload, capacitor failure due to resonance, and growing neutral current and voltage in the primary feeder are all possible outcomes of these harmonic pollutions in real-time distribution systems. Utility companies are interested in learning the current distortion levels at various residential system sites so that appropriate steps can be made to address this emerging concern. The issue can be solved via harmonic state estimation (HSE). HSE calculates the distortion level at additional unmonitored locations using the network model and harmonic measurements taken at monitored buses. Despite the efforts to solve the HSE issue at the distribution level, most of the research work suffers from a critical flaw that limits its capability. It is assumed that the measurement matrix is known, which explains how measurements relate to state variables. Since it is challenging to monitor the distribution network operating structure in real-time and to predict aggregated demands at load buses in the primary distribution network, this matrix is unknown in real-world circumstances. The study in [41] addresses this problem by improving the accuracy of HSE in unbalanced three-phase distribution networks through learning the measurement matrix from smart metering data. This article investigates the challenges of determining the spread of harmonic voltages in unbalanced three-phase power distribution systems. In this study, by utilizing data from smart meters, a data-driven strategy to HSE that deals with the uncertain measurement matrix is provided. Moreover, for networks that cannot be completely observed, it suggests a sparse Bayesian learning (SBL)-based estimator to find the harmonic sources and estimate the voltages with a great deal a smaller number of distribution-level phasor measurement units (DPMUs) than distribution nodes. In addition, through in-depth simulations, it is demonstrated that a PV linked to the main distribution network has no detrimental effects on the effectiveness of the suggested state estimator. In research [42], the HSE is formulated as a parametric interval linear system of equations

based on the weighted least squares (WLS) criterion. The issue of HSE of a power system whose network parameters are known to be within specific tolerance boundaries is addressed in this research. Interval numbers that indicate the outer bound of state variables are used to illustrate the solutions. Also, a technique is proposed for modifying the weight in WLS to consider for uncertain network parameters. The calculated bounds of the predicted state variables, both the real and imaginary parts, are shown by numerical experiments to encompass the estimated bounds produced by the Monte Carlo simulations. This information on the state variable boundaries shows the harmonic voltage level that exists in the power system when there is parameter uncertainty. When working with harmonic-related devices, e.g., harmonic filters, it offers helpful information. It also gives network operators the assurance that the true value does not exceed the system restrictions.

It is possible to identify the harmonic sources in a power system by calculating the harmonic components injected into the network by each source, load, or generator for all the harmonic orders of interest. The research in [43] has the main objective of the identification of the harmonic sources since it will enable system operators to take immediate action against the origin of the issue. This strategy is known as harmonic source estimation (HSoE). Due to the features of the issue (underdetermined systems because of a small number of observations and sparse state vectors), compressive sensing (CS) has been employed in the HSoE framework. This mathematical method circumvents the absence of power quality meters by enabling the recovery of sparse signals when only a few measurements are available. The identification of the primary harmonic sources in smart grids has led to the creation and investigation of a novel formulation of the P1-minimization method for CS issues, with quadratic constraint. For this situation, a novel whitening transformation is also suggested in this article which allows the energy of the measurement errors to be identified and estimated properly.

It is undeniable that HSE needs many synchronized monitoring equipment to thoroughly observe the network. Despite this, the lack of adequate monitoring infrastructure makes the application of HSE in distribution systems particularly difficult. A practical method for estimating harmonic distortions in residential distribution systems is presented in [44]. An integrated harmonic model is created for the secondary residential system after the measurement is initially made at several representative service (SRS) transformers. It is created by looking at the relationship between the harmonic injections of SRSs and active power. The utility network model is then used to develop a probabilistic harmonic load flow method. It is worth mentioning that the harmonic measurements that are now accessible are considered and thereby reducing the estimation uncertainty. To determine the system harmonic states while considering the data that are currently available, a probabilistic harmonic load flow (HLF) is further presented.

As mentioned before, the harmonic state estimation techniques need many power quality meters and mostly rely on the feeder's observability. They require historical data to increase observability and obtain pseudo measures. Practically speaking, many utilities' financial investments still prohibit them from allocating a significant number of power quality meters to address these restrictions. Additionally, sometimes not enough historical data or prior information is available to produce the pseudo measurements. A method based on the particle swarm optimization (PSO) algorithm that aims to calculate the harmonic source of three-phase real and reactive power as well as the magnitudes and locations of its current harmonics is proposed in [45]. It is worth mentioning that this strategy is different from harmonic state estimation techniques. The PSO method operates the harmonic source and location without estimating the harmonic states of all busses. It can be claimed that conditions such as harmonic source location and identification, the apparent power of the harmonic source and its distance from the meters have no impact on the proposed method. However, when the harmonic source estimated location is on a lateral branch bus, there was an impact on the identification.

An estimation technique for the localization of the source of harmonic emission in electrical distribution systems using a Bayesian technique has been proposed in [46]. The primary objective of this method is to alert the network management of any potential harmonic-producing loads and to give an estimation of the accuracy of such data. The behavior of the proposed harmonic source estimator and the analysis of harmonic propagation in unbalanced networks have been studied utilizing the single-phase equivalent network shown in Fig. 17 which consists of a power source (2.4 kV) and supplies five single-phase equivalent loads. The proposed Bayesian algorithm must estimate the values of a linear load (resistance and inductance in series) that is shunted by harmonic current generators to create the nonlinear load. The procedure's input data are derived from measured values, a priori knowledge, and an understanding of the system model. The magnitude of the 3rd harmonic current injected

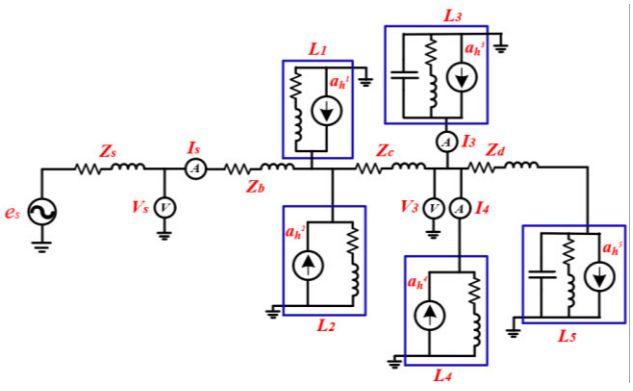

FIGURE 17. Equivalent single-phase network used in [46].

TABLE 8. Harmonic current injected by the loads.

	Currents injected by the loads (A)			
Harmonic order	*L2*	*L3*	*L4*	*L5*
3	3.961	6.646	13.516	13.753

TABLE 9. Operative conditions.

	L2	*L3*	*L4*	*L5*
Pseudomeasured Power (kW)	120.05	149.04	38.37	140.72
Pseudomeasured 3rd harmonic (A)	3.98	6.65	13.53	13.73
Actual 3rd harmonic (A)	4.15	0	0	9.87

into the network by the nonlinear loads when all nodes function in their nominal circumstances is shown in Table 8.

In the example test, the pseudo measurements have been used and the injected currents have been modelled as Gaussian distributions with a standard deviation of one-third of the expected values. The injected currents are also centered on the expected values, and proportional to the assigned power demand for each load and each harmonic order. In this scenario, all the loads are operating at their nominal power. While only *L2* and *L5* are nonlinear loads, *L1*, *L3*, and *L4* are linear loads. Fig. 18 provides a summary of the results related to the estimating procedure, and Table 9 presents the operative conditions for that case. The calculated harmonic current values are shown in Fig. 18 as black circles with the appropriate extended uncertainty. The blue squares represent the expected values, whereas the red triangles reflect the "actual" values.

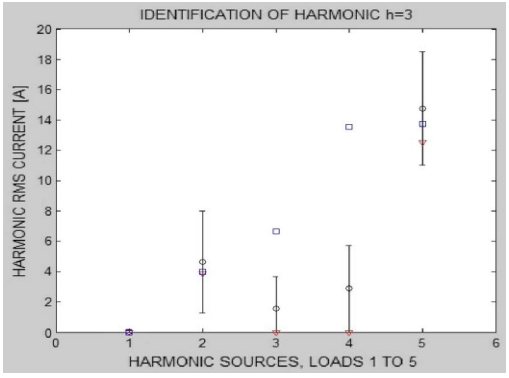

FIGURE 18. Estimation of 3rd current harmonic using the proposed method in [46].

Other studies have investigated the localization of nonlinear loads in distribution networks using the estimation technique. The technique proposed in [47] takes advantage of the limited real-time measurements that are existed in distribution systems as well as all other available information. This method offers a preliminary estimation of the current harmonics injected by the nonlinear loads along with an indication of the reliability of such information. An improved method using Metropolis-Hastings technique is proposed in [48] to achieve the posterior distributions of each Bayesian estimation method that was used in [47]. In this research, the harmonic sources are subsequently examined with uncertainty descriptions to estimate the current harmonics injected by nonlinear loads.

The Kalman filter (KF) and its variations are another popular real-time dynamic estimate technique. Linear KF and nonlinear extended KF are proposed to estimate the harmonic components of a noisy signal. A sliding-surface-enhanced fuzzy adaptive controller with a robust extended complex KF to estimate the frequency and amplitude of distorted signals in a power system has been utilized in [49]. Although the method performs well in steady-state tracking, it does not converge quickly enough following a sudden shift in frequency. The EKF also has the drawback of requiring the computation of power flow Jacobian matrices, which slows down implementation and affects real-time response. The research in [50] has been successfully utilized Unscented KF (UKF) estimation of linear and immediate frequency shifts in a balanced power system without harmonic emissions. The study in [23] describes a dynamic method for utilizing UKF to estimate the frequency and amplitude of unbalanced three-phase power systems with harmonics. By employing this technique, a nonlinear dynamic model of the three-phase voltage's complex form with harmonic content is provided, and a UKF is also used to estimate the magnitudes and frequencies of the fundamental component and its harmonics. When the voltage of a three-phase unbalanced power system comprises the fundamental, the 2nd, and the 3rd harmonics, whose amplitudes fluctuate continuously or suddenly, step and linear frequency changes are applied to the model to evaluate how well the suggested UKF frequency estimation method operates.

The grid voltage harmonics can be reduced with the help of the Renewable Energy Source (RES), but first, these harmonics must be estimated. The harmonics must be calculated in the *dq* rotating reference frame for efficient harmonic injections. Therefore, it is desirable to create harmonic estimators that provide their outcomes in the *dq* reference frame. Most of the techniques for estimating the single-phase voltage harmonics in the *dq* reference framework have two steps. The first stage includes filtering the harmonic components, and the filtered harmonics are then converted into the *dq* reference frame in the second stage. However, the filtering stage slows down the estimating process and increases processing complexity. A technique for estimating the harmonics in the *dq* reference frame and for performing processing with less than half the mathematical operations needed by the traditional methods is proposed in [51]. Additionally, the estimator's transient response is faster than that of the standard methods. Before transferring the sampled grid voltage to the PLL block used to estimate the grid phase, the harmonics are eliminated to speed up and improve the accuracy of the harmonic estimation process.

The windowed FFT algorithm, which is employed to estimate harmonic parameters in a power system is extremely

susceptible to spectral leakage and the picket fence effect. Particularly, the polynomial fitting always includes the even components, which might add to the computational complexity. In [52], a symmetrical interpolation FFT technique based on the Triangular Self-Convolution Window (TSCW) to eliminate the even terms in polynomial fitting is proposed to reduce these undesired effects. The proposed technique outperforms previous Windowed Interpolation FFT (WIFFT) algorithms because the fitting polynomials only contain odd terms and are simple to implement in embedded systems, while the TSCW exhibit favorable sidelobe behaviors and significantly reduces leakage error. A differential equation is used to provide a symmetrical approximation estimation of the harmonic amplitude that minimizes the contribution of leakage of negative frequencies to the fundamental component. Significant leakage errors and harmonic disruptions can be removed by weighted samples with the TSCW for the window's high sidelobe decay rate and low peak sidelobe level.

Previously, the single-phase converter-based loads are modelled as harmonic current sources with fixed magnitudes. However, this technique causes a significant harmonic current overestimation due to the attenuation and diversity effects of the loads when the combined effect of these loads is evaluated. Harmonic analysis can be used for other devices and any voltage levels; however, it becomes difficult to determine the circuit parameters (R, L, and C in a diode rectifier) for each load because they are created by different manufacturers and have their own designs that can be developed from the fundamental circuit. To estimate R, L, and C in the equivalent circuit, [53] suggests a measurement-based method. According to this research, the R, L and C parameters can be estimated after measuring the current waveform at any given voltage, and the acquired equivalent circuit can be further developed to complete harmonic analysis under any voltage distortions. It is also widely known that a frequency-domain harmonic model must be used for harmonic load-flow research. As a result, this research suggests a model based on a generic harmonic frequency-domain using the estimated circuit parameters.

Rapid frequency fluctuations cause grid instability and make it possible for grid components to be damaged or even destroyed by significant harmonic distortions of voltages and currents. Therefore, it is essential to identify and estimate fundamental and higher harmonic components in real time as quickly and accurately as possible. This is necessary to be able to take appropriate action to improve system stability and power quality and compensate for the deteriorated operating conditions. Traditionally, Fast Fourier Transformation (FFT) has been used to analyze and estimate a signal with significant harmonic distortion; however, this method needs a relatively long computational time and a substantial amount of data to be processed. For signals with considerable harmonic distortion, well-known and very fast techniques are proposed, e.g., parallelized second order generalized integrator (SOGI). As a result, [54] suggests a modified second-order generalized integrator (mSOGI) technique that accomplishes a required estimate process settling time for a fast estimation of all harmonic components of arbitrarily distorted voltage and current signals in power systems. All harmonic components of interest can have their amplitudes, angles, and angular frequencies estimated in real-time by the proposed method. The parallelized modified SOGIs tuned by pole location make up the suggested algorithm. The modified SOGIs include extra feedback gains that give them the required degrees of freedom to guarantee the preferred settling time. A modified frequency-locked loop (mFLL) with gain normalization, sign-correct anti-windup, and rate limitation is used in combination with harmonic estimation for time-varying fundamental frequencies.

Based on the use of phasor measuring units (PMUs), the fundamental component synchro-phasors are now widely used in many electrical power system applications. While the development of harmonic synchro-phasor estimation technologies is difficult, it is still achievable if the harmonic phasor, e.g., the magnitude and phase of each harmonic component are accurately estimated, especially in situations where there is noise and frequency variation. A pre-processing algorithm for the DFT called B-spline-based interpolation is proposed in [55]. The performance is assessed in terms of total vector error (TVE) and IEEE C37.118.1 and IEC 60255-118-1 standards tests. Moreover, the proposed method is compared with four different harmonic phasor estimation (HPE) methods, including the Taylor-Fourier transform (TFT), flat-top finite impulse response (FT FIR), and sinc interpolation function-based estimator (SIFE). Under large frequency deviation, the proposed technique can deliver a TVE of less than 1% for all harmonic phasors, from the 1st to the 50th order. The main contribution is to demonstrate that a good resampling algorithm used in association with the classical DFT is a method that ensures high-quality phasor estimations that meet PMU criteria.

By expanding the single-phase frequency estimator, the harmonic A&M (HAM) estimator is created to estimate the voltage frequency in a balanced three-phase grid utility. However, the initial poor estimation of the harmonic waveforms is the main flaw in the HAM technique. To further enhance the parameter estimation from the HAM step, the weighted least squares (WLS) refinement step makes use of the harmonic and interharmonics correlations in [56]. The HAM-WLS framework is a novel two-step framework which will improve the HAM estimator and include a new WLS phase stage. The resultant HAM-WLS approach can also be used to evaluate many power signal models, including single-phase, unbalanced three-phase, harmonic, and interharmonics instances. After employing a harmonic variation of the HAM estimator, a WLS estimator further enhances the estimations of the fundamental frequency and phase. Therefore, the recommended HAM-WLS technique offers accuracy even in electrically noisy environments that are further polluted by harmonics and interharmonics.

The contribution of iron and steel (I&S) plants supplied from a PCC to current harmonics is estimated using a state estimation-based method in [57]. The suggested technique separates the harmonic current contributions of loads from the upstream effects using sample-by-sample time-synchronized field measurements of load currents and voltage signals. Additionally, it depicts the nonlinear properties of the utilities and plants as harmonic current sources. Because this approach is dependent on the field measurement, it is necessary to decrease the measurement errors of traditional voltage transformers at harmonic frequencies. The harmonic contributions of all plants are calculated using the estimated harmonic voltages and currents, the Norton equivalent circuits of the plants, and the Superposition theorem. The outcomes have demonstrated that the suggested approach can be applied as an estimation tool to identify the harmonic current contributions of all I&S plants receiving power from the PCC. While simultaneously reducing the Gaussian measurement error of conventional voltage and current transformers, the proposed method eliminates the need for resistive-capacitive voltage transformers, which are expensive and inconvenient to use for accurate harmonic voltage measurements. As a result, it provides accurate estimates of the harmonic contributions of the electric arc furnace plants.

B. NON-PARAMETRIC HARMONIC ESTIMATION METHODS

The main goal of the strategy proposed in [58] is to identify key locations for the installation of the meters. As a result, the calculated values for the other state variables should solely consider the network parameters (impedances and admittances). Aside from the anticipated changes in shunt admittances and series impedances that the frequency would bring about in the network parameters, no more specific harmonic effects should be considered in accordance with the suggested technique. Since there is no approximation procedure, this approach does not bring errors into the estimating process. Only the measurements and network parameter calculations are subject to inaccuracy, which could have an impact on the outcomes of other conventional methods for estimating harmonic states. The technique worked remarkably well for estimating harmonic state variables. Furthermore, the proposed harmonic methodology can still be utilized to precisely identify the harmonic sources because it incorporates voltage and current state variables.

The technique used in harmonic distortion state estimation (HDSE) is the opposite of a simulation process. When the power system responses are provided by a set of data, estimators analyze the harmonic injections while simulators estimate the power system response to harmonic injection in one or more locations. The HDSE approach creates an effective and affordable tool for PQ monitoring systems to employ harmonic distortions estimate over the entire network. The network topology related harmonic frequency admittance matrices, passive (linear) loads, and the positions and measurements of PQ meters serve as the foundation for the HDSE algorithm. The HDSE of the network is a challenging problem because it requires the use of minimal and reliable data from a few numbers of PQ meters. There might be differences between the real and simulated systems due to a variety of factors. In addition to meter calibration, concerns including data transfer and network data reliability are also crucial. The synchronization data from several PQ meters is another significant issue that should be considered. Evolutionary strategies (ES) are fascinating solutions due to their simple implementation, especially when simulation algorithms for the special problem are established. Based on measurements taken at a few specific sites, [59] introduces a novel approach for estimating harmonic distortions in a power system. This method makes use of evolutionary strategies (ES), a development subset of evolutionary algorithms. The major benefit of employing the proposed method is its modeling capabilities in resolving complex problems. The above-suggested problem-solving algorithm uses data from multiple PQ meters, which can be synchronized by advanced technologies such as global positioning system devices or by employing data from a fundamental frequency load flow. It is worth noting that the suggested technique can be utilized for all pertinent harmonic orders and the THD of any network bus can be estimated.

A traditional technique for estimating grid voltage parameters also referred to as the phase-locked synchronous reference frame (SRF-PLL), has been utilized extensively in industry. However, the growing use of Renewable Energy Sources (RESs) and the existence of numerous nonlinear loads in modern networks frequently result in harmonic disturbances and grid instabilities. An adaptive observer-based closed-loop feedback system technique for estimating the fundamental and harmonic frequencies, amplitudes, and phase angles of the three-phase grid voltage is suggested in [60]. This estimating method is based on the time domain but does not rely on PLL, quadrature signal generation (QSG), or sophisticated filtering. By employing observer theory and adaptive estimation techniques, the steady-state inaccuracy can be kept at zero. The proposed adaptive estimating technique is robust to harmonic voltage disturbances and grid unbalanced failures because of the nature of its closed-loop feedback system. Additionally, it guarantees that there is no steady-state inaccuracy even when the three-phase grid's fundamental frequency deteriorates and drastically deviates from its nominal value.

Synchronous sampling is challenging to implement because of the typical power frequency variability. Therefore, when employing the Fourier transform, the inevitable products, such as spectrum leakage and the picket fence effect will have a substantial impact on the accuracy of harmonic analysis. To cope with this issue, a unique approach for power system harmonic estimation called frequency shifting and filtering (FSF) algorithm is proposed in [61]. According to this method, the frequency of the sampled signal is first shifted by the generation of a reference signal. Then, the spectrum interferences are removed using an iterative averaging filter.

Finally, a precise harmonic estimation can be accomplished because only components that are important are kept. The primary goal of the proposed algorithm is to shift each of the desired components to 0 Hz before removing spectral interferences using an average filter. The process of the proposed algorithm for harmonic estimation is shown in Fig. 19.

Applications for harmonic phasor estimation in the protection and monitoring of power systems include HSE, high-impedance fault identification, and islanding detection. The fact that distinct harmonics have different harmonic frequency bandwidths presents a significant difficulty for harmonic phasor estimation. Therefore, a harmonic phasor estimator (HPE) that can adjust these differences is necessary for the estimation process. Despite the sinc interpolation function-based estimator (SIFE) has this capability, it has two drawbacks: 1) it requires multiple simulations to choose the model parameter, and 2) it is unable to produce results with 0% error under nominal frequency conditions. As a consequence, an unique HPE is put out in [62] that is based on the frequency-domain sampling theorem and uses numerous fictitious exponential functions to represent the harmonic phasor. The proposed HPE and SIFE are compared in terms of frequency response, model parameter selection methodology, and simulation testing. The outcomes demonstrate that the suggested HPE has the benefits of being an easier method for selecting model parameters based on the fundamental frequency bandwidth, which can be determined based on previous observing data. In addition, this method has zero-error outcomes for nominal frequency circumstances and gets greater accuracy for harmonic frequency deviation and harmonic modulation situations [62].

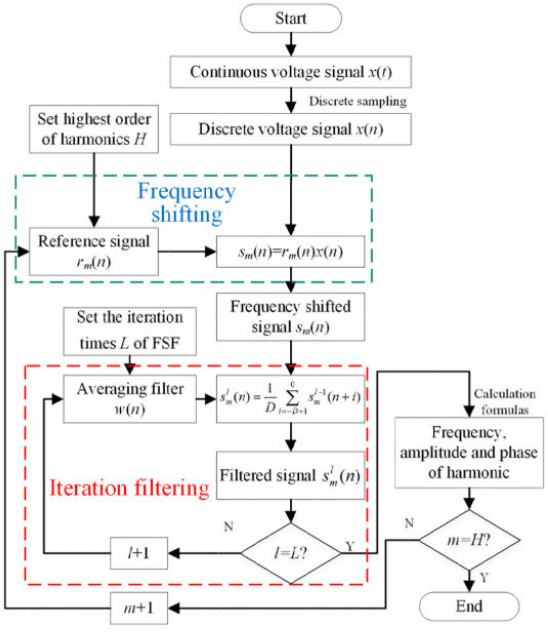

FIGURE 19. Flowchart of the proposed harmonic estimation algorithm in [61].

A fast-converging optimal technique to estimate the harmonic components of a time-varying signal online is proposed in [63]. The application of the estimator to provide reference signals for an ideal control system to suppress the harmonics components is also examined in this paper. The proposed approach considers real-world assumptions including the presence of time-varying harmonics and noise in the signal to be investigated without assuming steady-state conditions. The harmonic estimator application involves two practical tests: the ideal estimation of the harmonic components of the current waveform in a nonlinear load, and the use of harmonics data to suppress the harmonics through an APF. The proposed optimal harmonic estimator is a signal-processing-based approach, which involves designing and adapting a harmonic model online using measurements of the variable that must be decomposed in terms of harmonics. Because the harmonic components have been estimated in the time domain, no additional computation is needed to convert the signal to the frequency domain.

In a power system network where harmonics exist, to estimate the frequency, a novel DFT-based approach is proposed in [64]. It is worth noting that the Discrete Fourier Transform (DFT)-based technique is the most popular among these methods since it is easy to apply and has a high level of precision. The DFT-based technique employs DFT to determine the phasors of two consecutive data frames while assuming the fundamental frequency. The frequency deviation between the real frequency and the assumed frequency is then calculated using the difference in the phase angles between the two phasors, and lastly, the actual frequency can be estimated. The suggested approach also takes the fundamental frequency and after creating a new sequence using the summation of the samples from the original sampling sequence, the frequency deviation value is calculated using the amplitude ratio between the new and original sequences. The impacts of interharmonics, harmonics, and negative fundamental component effects are also investigated. A preprocessing method is also suggested to get rid of the impacts of the interharmonics with a frequency close to the fundamental frequency. The suggested method can be utilized for online frequency estimation in harmonic-polluted environments due to its high harmonic resistance and the required low processing effort.

Traditional-based harmonic estimation techniques lack high efficiency, quick response, and precision and their application is limited. In this case, Artificial Intelligence (AI) techniques are recently introduced because of their big impact on power electronic devices and motor drives. AI techniques are superior to the traditional methods because of their accuracy, precision, and the ability to respond quickly, which will be described in the next section.

V. ARTIFICIAL INTELLIGENCE BASED HARMONIC ESTIMATION TECHNIQUES

Artificial Intelligence (AI) aims to simulate human intelligence processes through computer systems. AI develops

systems that are capable of reasoning based on observations and can act accordingly.

A. FUNDAMENTAL CONCEPT OF ARTIFICIAL INTELLIGENCE

There are numerous branches within AI, including robotics, machine learning and expert systems. Machine learning is a sub-filed within AI that enables machines to automatically learn from past data without being explicitly programmed. Deep Learning, which is a sub-field within machine learning develops artificial neural networks for representation learning from the data. Fig. 20 visually illustrates the organization of these concepts.

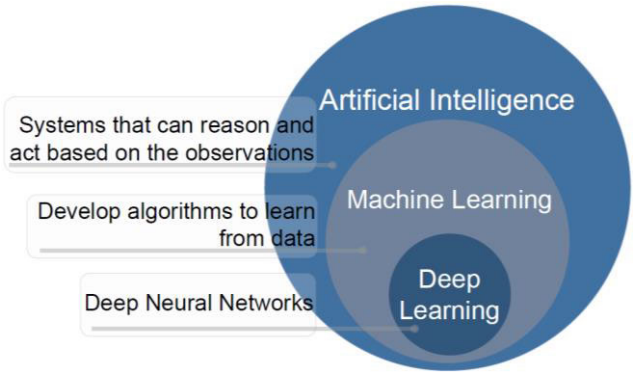

FIGURE 20. Organization of Artificial Intelligence, Machine Learning and Deep Learning Concepts.

1) MACHINE LEARNING

Within the last two decades, we have seen an explosion of data and numerous machine learning algorithms have been introduced to find the patterns that are hidden within the mass amount of data generated [65], [66]. There exists a clear distinction between traditional computer programs and machine learning. The former applies human-defined rules to the data and generates outputs for a certain task while the latter leverages data and the target outputs and discovers the rules behind that task. To uncover the underlying governing phenomenon, the algorithm passes through an iterative learning process, where different rules are tested to evaluate their performance. Once the learning process discovers the best rule, it is used as the solution to the target task. Numerous approaches have been introduced to perform learning and these approaches can be broadly categorized into supervised learning, unsupervised learning, semi-supervised learning, and reinforcement learning-based algorithms. Prior to illustrating the differences between these classes of algorithms, we would like to first clarify the following terminology:

- **Dataset**: A collection of examples that are obtained from the task that we are interested in solving.
- **Features**: Characteristics or attributes within the data that the machine learning algorithm utilizes in training.
- **Label**: A designation given to a certain example within the dataset to tag its certain properties or characteristics. A label is used as a classification to recognize the target class of the input data in supervised machine learning.
- **Model**: The internal mechanism that the machine learning algorithm has learned. It describes how inputs are mapped to the outputs and the rules that govern this mapping.

The distinction between supervised and unsupervised learning arises due to the differences in the way that inputs and outputs are used inside the algorithms. Specifically, in supervised learning, the data is fed to the algorithm as input and output pairs and during the learning process, the model learns a mapping from inputs to the outputs. As such "supervision" is provided by the outputs, hence, the term supervised learning. In contrast, in unsupervised learning, only the input data is provided to the algorithm, and no outputs (or labels) are given. The unsupervised learning algorithms try to find similarities and dissimilarities within the given data and uncover hidden patterns within the input data.

Semi-supervised learning can be seen as a combination of supervised and unsupervised learning approaches. Specifically, the datasets that semi-supervised learning algorithms leveraged contain a large amount of unlabeled data and a small amount of labeled data. As such, a combination of supervised and unsupervised learning theories is utilized to solve the problems within the semi-supervised learning domain. Reinforcement learning follows the conceptual framework that we as humans learn in our everyday life. The human learning process is governed by positive and negative feedback that reinforces our behavior. Similarly, in reinforcement learning algorithms, the behavior of the model is optimized such that the expected reward for behavior is maximized. In the following sections, we describe popular types of machine learning models that have been introduced.

2) ARTIFICIAL NEURAL NETWORK

One of the pivotal developments within machine learning is the Artificial Neural Network (ANN). This is an architecture that has existed from the beginning of the machine learning domain, however, with the success of deep learning, ANNs are becoming increasingly popular. ANNs are inspired by the human cognition process and utilize a collection of neurons to map the input to the outputs. Specifically, the neurons are interconnected and within each neuron, there is an input receiver, input processor, and output transmitter. Fig. 21 visually illustrates these functionalities.

Specifically, the transmitted output, y, can be written as:

$$y = f(\sum_i w_i x_i), \tag{15}$$

where, x_is are the inputs to the neurons and w_is are the weights that map the input to the output. Here, the function f is an activation function [67], [68] which is used to add nonlinearity to this mapping. Sigmoid, tanh, linear, and rectified linear units are some popular activation functions. In addition to these parameters, a neuron is usually equipped with a bias term, a constant which allows a shift of the activation.

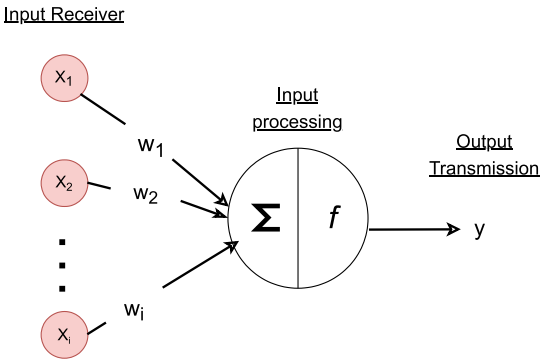

FIGURE 21. The main components of an artificial neuron that consists of input receiver, input processor, and output transmitter.

However, for simplicity of the illustration, we do not utilize this in our formulation. The popularity of ANNs comes from their ability to solve challenging problems and this owes to the ability of ANN architecture to model complex non-linear relationships using its hidden layers. Specifically, with deep neural networks, which is a sub-field within machine learning which specifically focuses on ANNs that have deep layer structures, multiple hidden layers are stacked together to form a deep ANN architecture. Fig. 22 shows a deep neural network architecture that has two hidden layers. The learning process of ANN happens in two stages, namely feedforward and backpropagation. In the feedforward stage, the outputs are generated from the network based on the current set of network parameters (i.e., weights and biases). This is the same as the illustration that was provided in the case of a neuron, however, in the case of a neural network, the process is repeated through all the neurons in all the layers, namely, the input layer, hidden layer, and output layer.

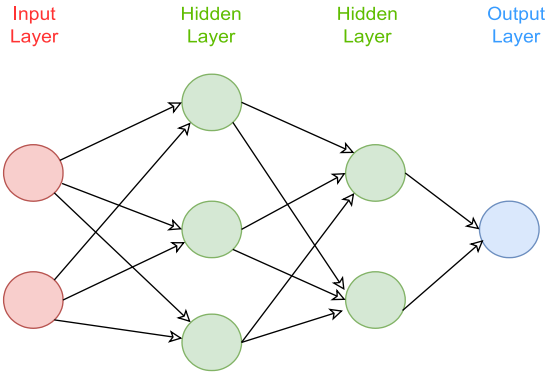

FIGURE 22. A Deep neural network with two hidden layers.

After receiving the network output, the next process is error backpropagation. For the calculation of the error for backpropagation, depending on the task, different loss functions are used. For instance, for classification tasks loss functions such as cross-entropy loss [69] are used while mean squared error loss [70] and the sum of squared error loss [71] are used for regression tasks. The backpropagation focuses on updating the network parameters that were used in the forward propagation such that the error between the target output and the network output is minimized. For this parameter update procedure optimization algorithms are utilized together with loss functions. The optimization algorithm dictates how the individual network parameters are updated by the calculated gradients of the error. Some popular optimization algorithms are Adaptive Moment Estimation (Adam) [72], RMSProp [73], and Stochastic Gradient Decent (SGD) [74]. Once this update is complete, the network has completed its first iteration through the training process and enters the next iteration. This process is repeated until a stop criterion is reached. A maximum number of iterations, a minimum loss threshold, or model convergence is usually used to define a stop criterion.

3) 2D CONVOLUTION NEURAL NETWORKS

The Convolution Neural Network (CNN) is inspired by the organization of the human visual cortex. The CNNs are specially designed for image data and learn a set of task-specific filters (or kernels) that can extract relevant information for the task at hand. They reduce the number of trainable parameters in the network by sharing the filters (Fig. 23).

First, the kernel is placed on top of the image, and values of the pixels that encompass the kernel are multiplied by the weights in the kernel and depending on the aggregation function, a summary statistic is propagated to the next layer as the feature of that pixel patch.

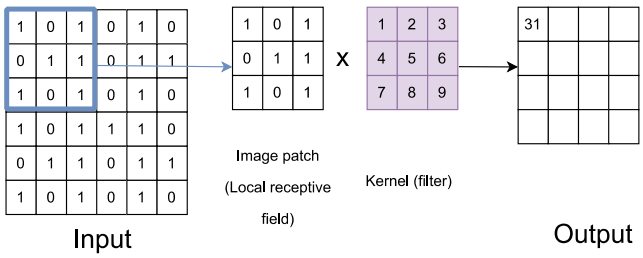

FIGURE 23. Illustration of the convolution operation applied over an input image.

Then the kernel shifted over the image and the length of this shift is determined by the parameter stride. For example, the kernel is shifted only a pixel when the stride is 1, however, if the stride is set to 2 it is shifted two pixels to the right. The process is repeated until the entire image is visited using the kernel and multiple kernels are utilized to learn multiple feature representations. Subsequently, the pooling operation is applied to combine and compress the extracted features from the convolution operation. Furthermore, the pooling operation lets the recognized features to be independent of their location in the image. For example, a 2×2 max-pooling operation would propagate only a maximum of the 4 values in the region that it encompasses. Finally, in a convolution neural network, a flattening operation is used to convert the resultant 2-dimensional feature vector from the convolution and pooling operations into a linear vector, which

is subsequently passed through a classification sub-network to generate the necessary classifications.

4) RECURRENT NEURAL NETWORKS

The Recurrent Neural Networks (RNNs) method can be used when modeling time series data recurrence is a critical characteristic. In the feed-forward neural network that was discussed in the previous section, there exists only a single directional flow of data. In contrast, in RNNs the output of the current time-step is also passed as the input to the next time-step. As such, there exists a recurrence within the neural network architecture. The structure of the RNN allows it to maintain a notion of time within the network and for the clarity of the illustration, Fig. 24 temporally unrolls the RNN architecture.

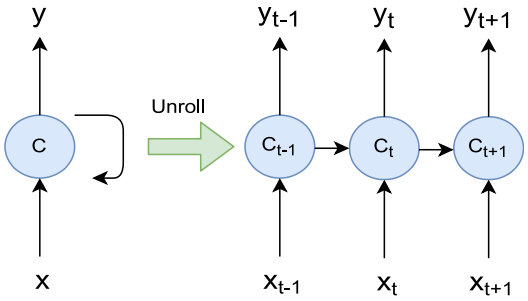

FIGURE 24. Illustration of Temporal Unrolling procedure of Recurrent Neural Networks.

Specifically, in RNNs, the gradient of the error at a particular timestep depends upon the predictions at the previous timestep, hence, the error backpropagation procedure is termed as Backpropagation Through Time (BPTT). The process of BPTT suffers from vanishing gradients [75] when the length of the input time-series is larger, therefore, RNNs are in efficient to model lengthy sequences.

5) LONG SHORT-TERM MEMORY NETWORKS

As a solution for the vanishing gradient problem, Long Short-Term Memory (LSTM) networks are proposed by Hochreiter et. al. in [76]. LSTMs leverage a concept called ''memory cell'' to store information that are relevant to the prediction. Specifically, a series of gated operations were proposed to manipulate the stored information within the memory and to effectively utilize the information without losing them when the modeled time-series becomes too long. Three gate functions, namely, forget gate, input gate, and output gate are utilized in the process. An LSTM cell structure is schematically illustrated in Fig. 25.

First, the forget gate determines the portion of the content from the previous timestep that should be retained and the portion that should be forgotten. As such, this gate controls the information flow from the previous time step to the current input. The gate value range between 0 and 1 where 0 indicates everything is forgotten and 1 indicates that everything

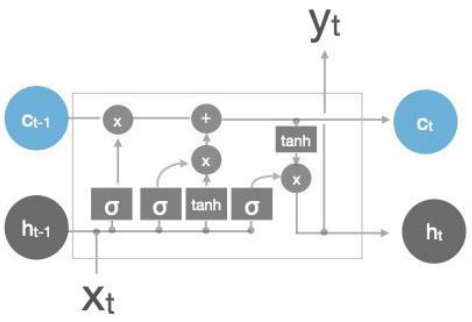

FIGURE 25. Schematic illustration of Long Short-Term Memory cell. Recreated from [77].

is passed through. This can be written as:

$$f_t = \sigma\left(w_f\left[h_{t-1,}x_t\right] + b_f\right), \tag{16}$$

where w_f and b_f are the weights and bias, h_{t-1} is the previous time step's output and x_t is the current input and σ is a sigmoid function. In the next step, the portion of the information that should be written to the cell memory is decided using the input gate. This can be computed as:

$$g_t = \sigma\left(w_i\left[h_{t-1,}x_t\right] + b_i\right), \tag{17}$$

and the function *tanh* is used to determine the information that should be written as:

$$\dot{c_t} = \tanh\left(w_c\left[h_{t-1}, x_t\right] + b_c\right). \tag{18}$$

The cell state is updated using,

$$c_t = f_t \times c_{t-1} + i_t \times \dot{c_t}, \tag{19}$$

and the output gate controls what information is passed as the output of the current times step. This can be written as:

$$o_t = \sigma\left(w_o\left[h_{t-1,}x_t\right] + b_o\right), \tag{20}$$

and the current time step's output is given by:

$$h_t = o_t \times \tanh(c_t). \tag{21}$$

6) TEMPORAL CONVOLUTION NEURAL NETWORKS

Temporal Convolution Neural Networks (TCNNs) have recently outperformed recurrent neural networks in numerous sequence modeling tasks [78] due to their improved memory retention. TCNNs can attend to the entire input sequence when making a prediction, rather than the information from the current time step which RNNs attend to. In Fig. 26, visualize the 1D convolution operation where the output is generated using the dot product between the input elements within the window and the kernel weights. Fig. 27 illustrates the concept of dilation which is the distance between elements in the input window that are considered when generating an entry in the output sequence. Dilation allows the modeling of relationships between distant elements in the input sequence without the need to stack multiple layers.

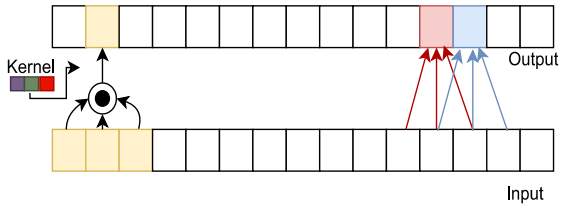

FIGURE 26. 1D convolution operation and the flow of information from input to the output. Recreated from [78].

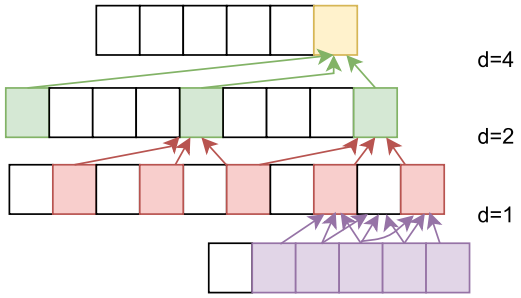

FIGURE 27. Visual illustration of dilation. Recreated from [78].

7) SUPPORT VECTOR MACHINE

Support Vector Machines (SVMs) are another type of machine learning model that is highly preferred due to their greater robustness despite lower computation burden. Like ANNs the SVMs can also be used for both classification and regression tasks. The SVM model learns to find a hyperplane in the N-dimensional space (where N is the number of dimensions in the input features) that maximizes the distance between the data points of different classes. As such, the hyperplane is the decision boundary that helps the classification of the data points and SVM utilizes support vectors, which are the data points that are closer to the decision boundary to influence the position and orientation of the hyperplane. The objective of the SVM algorithm is to maximize the margin between the data points and the hyperplane and it uses hinge loss [79] to maximize this objective. When the data is linearly separable, as shown in Fig. 28, it is easy to define a hyperplane, however, is far more challenging when the data is non-linearly separable. SVM utilizes kernels such as polynomial, radial basis function, or sigmoid to map these non-linearly separable data points to higher dimensional space in which the data is linearly separable.

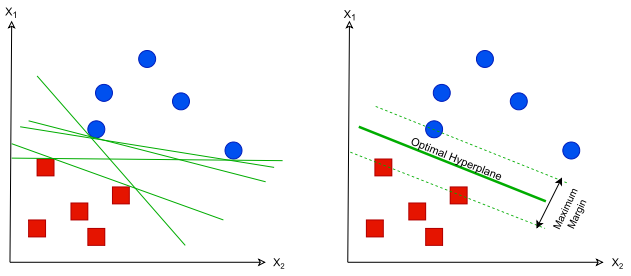

FIGURE 28. Definition of Hyperplanes. Recreated from [80].

B. ARTIFICIAL INTELLIGENCE-BASED HARMONIC ESTIMATION TECHNIQUES

Nowadays, modern power electronics are being used more often to create harmonics in power system networks, which eventually undermines their standard performance in terms of losses, breaker failure, and equipment malfunction. Recently, many converters are employed in power systems in which their cumulative contribution to harmonics goes beyond a simple addition. As a result, the analytical techniques employed to determine and accurately measure the real number of harmonics are ineffective. Statistical techniques such as the Unscented Transform (UT), Monte Carlo Simulation (MCS), and others can be used to solve this difficulty, but their computing costs and time requirements are quite high.

Utilizing Machine Learning (ML) approaches, such as fuzzy logic, neural networks, and Principal Component Analysis (PCA), for effective harmonics estimate with manageable processing demands, is another option. While unsupervised machine learning (such as classification and clustering) gives the trend of occurrence rather than a particular output, supervised machine learning correlates the input with the output. The ML approaches can be used to generalize various power system configurations as well as to enhance the hyper-parameters of data models and provide an abstract representation of source data, both of which are required for the signal processing of harmonic contents in a condensed subspace.

According to the signal processing of power quality in the harmonic domain, the origin of harmonics is due to deviation in waveshape from its fundamental frequency component. A novel framework for harmonic estimation and classification utilizing ML techniques is presented in [81]. The harmonic contents of the voltage and current signals are initially estimated using a shallow neural network and fuzzy logic systems. The estimation of harmonic content is accomplished using the sequence components and Individual Harmonic Distortion (IHD) level of the source signals. The explainable convolutional neural network (xCNN) is then trained for harmonics classification using the outputs from the neural and fuzzy systems. The standard binary support vector machine (SVM) is trained for harmonic classification using the pertained ALEXNET network, which is a component of the xCNN. Artificial Neural Network (ANN) is essential for parameter estimation since it receives input data and propagates from layer to layer to produce the output. The weight and bias of every signal originating from the former layer are combined in each linked neuron. The activation function and convolution of two signals are used to create the output, as shown in Fig. 29. The provided ANN is referred to as a shallow neural network because there is just one hidden layer in it. Fuzzy logic is created through four fundamental processes which are declaring the input and output variables,

selecting the membership function, creating the corresponding rules, and the defuzzification of the result. Fig. 30 depicts the conceptual diagram of developed fuzzy logic.

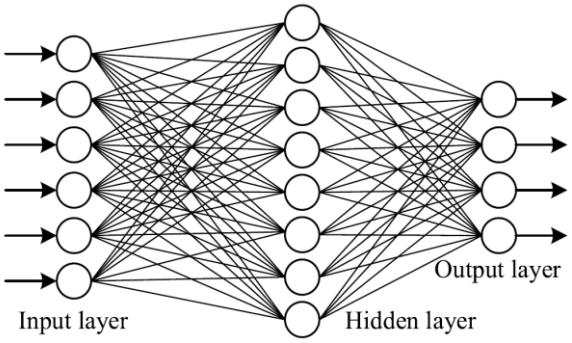

FIGURE 29. Shallow neural network [81].

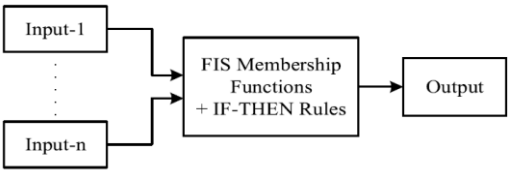

FIGURE 30. Conceptual diagram of fuzzy logic technique [81].

For generation and transmission to operate smoothly and without interruption, power system operators implement high Power Quality (PQ) criteria to ensure that harmonics produced by industrial and commercial customers must be filtered into an acceptable range. Passive filters have traditionally been employed to reduce these PQ-related problems. Therefore, Active power filters (APFs) introduced as an effective solution for reducing harmonic-related issues and have become increasingly popular because of their adaptability and capacity to correct for harmonics, imbalance, and reactive current. The advantage of active filter over passive is due to better performance over a wide frequency range.

There are two types of methods for calculating customer and network harmonic contributions at a point of common coupling (PCC) which are techniques based on measurements and techniques that use harmonic modelling. Only the harmonic voltages and currents that have been recorded are used in the measurement-based approaches. To evaluate harmonic sharing at a PCC, the operators do not need to measure the load and network impedance. It is worth noting that the harmonic contributions are computed using the observed values at a PCC and the network and load modelling techniques based on harmonic modelling. Norton and Thevenin equivalent circuits can be used to model the network and the consumer at each harmonic order. The grid utility harmonic impedance can be estimated using a variety of techniques which are based on Intrusive and Non-intrusive methods. Invasive techniques rely on introducing deliberate system disturbances and using transient currents and voltages. These techniques provide outcomes with acceptable precision. However, their employment is restricted due to the detrimental effects of deliberate disturbances on network performance, short measurement times, the challenges of implementation, the impossibility of tracing impedance changes, and the requirement for high-speed acquisition systems. On the other hand, the grid harmonic impedance at a PCC can be determined using non-invasive techniques, without the use of any disturbances, and simply by measuring harmonic voltage and current changes. The benefits of non-invasive approaches over invasive methods include simplicity, the possibility to deploy using inexpensive PQ analyzers, and frequent tracking of the impedance changes. However, the fundamental drawback of non-invasive approaches is their susceptibility to background harmonic changes, which lowers their accuracy, validity, and dependability, especially for higher-order harmonics. A brand-new, non-intrusive technique for calculating utility harmonic impedance is proposed in [82]. Since background harmonic fluctuations are the main source of uncertainty for non-invasive procedures, appropriately measured samples are chosen using a three-point data selection methodology to improve the method's accuracy. The utility harmonic impedance at PCC is then evaluated using a novel non-invasive approach based on fuzzy logic. The constrained recursive least squares algorithm (CRLS) is modified in the proposed technique by incorporating fuzzy logic into a collection of fuzzy if-then rules. To estimate the utility harmonic impedance because of changes in quantities at PCC, these approaches are utilized to compute the amount of the CRLS forgetting factor.

When it comes to harmonic/interharmonics estimation, model-based parametric approaches have numerous benefits over traditional discrete Fourier transform (DFT)-based procedures. However, high computational demands limit its use in offline analysis. The accuracy and computation time for harmonic/interharmonics optimization of stationary and non-stationary power supply signals are proposed in [83] using an estimation of signal parameters adaptable approach based on the rotational invariance technique (ESPRIT). This technique determines the model order (the number of sinusoids in the distorted power supply signal), and then it modifies the auto-correlation matrix dimension in accordance with the reconstruction error. Moreover, to significantly reduce computation time while maintaining accuracy in harmonic estimation of stationary and nonstationary power signals, Sliding Window ESPRIT (SWE) method is proposed to estimate the model order in each data block and then optimizes the dimension of the autocorrelation matrix (ACM). The proposed technique also can calculate the actual harmonic and interharmonics frequencies, amplitudes, and phase angles of stationary and nonstationary signals.

To give a more precise and robust estimation of harmonics and interharmonics, [84] provides an approach for accurate model order estimation (the number of frequency components), which is employed in the estimation of

signal parameters via rotational invariance technique (ESPRIT). The frequency, amplitude, and initial phase angles of the distorted supply can all be calculated using the suggested approach which first uses the Relative Difference (RD) plot to determine the number of frequency components contained in the signal. Additionally, it avoids the need for very high-order basic component filters and their negative effects. To identify the frequency components that are present in the signal, ESPRIT uses an eigenvalue decomposition-based batch processing approach.

The real-time estimate of moderately time-varying harmonics of voltage/current signals is presented in [85] as a quick and precise method. The suggested methodology relies on the rotational invariance technique (ESPRIT)-assisted adaptive wavelet neural network signal parameter estimation (AWNN). The ESPRIT complements the AWNN to handle time-varying signals more accurately while still providing rapid estimates of the prominent harmonics. The proposed method can estimate the main harmonics of the signals precisely when the time is varying. The suggested technique also makes use of the idea of learning on the fly to take advantage of AWNN's learning capabilities and enhance its performance for time-varying inputs. Fig. 31 depicts the proposed method's concept. The data acquisition (DAQ) system is used to acquire the signal, and two parallel processing channels are used to process it. Process 1 uses the AWNN to estimate harmonics in real-time, whereas Process 2 monitors and trains the AWNN's parameters. The set of input-output pairs necessary for training the parameters cannot be produced with merely half-cycle data points; consequently, enough data points are gathered in the data buffers and examined using the ESPRIT tool.

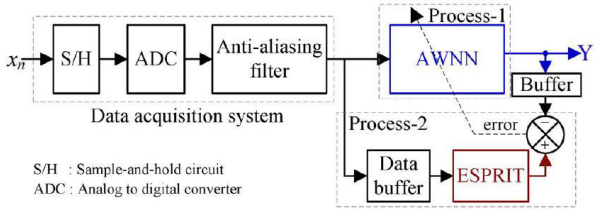

FIGURE 31. Conceptual block diagram of the proposed EA-AWNN method [85].

Using the measurements at other buses and lines, the HSE techniques can provide the estimation of current and voltage harmonics from the harmonic sources which are not monitored. Therefore, the HSE needs to be analyzed and investigated as a frequency domain concept. It is worth mentioning that the traditional signal processing methods e.g., ST, FT, and WT can be utilized to transform signals from the time domain to the frequency domain; however, their application in HSE issues is limited. In fact, conventional methods can only be used to identify harmonic content at buses when time domain measurements have been performed, whereas HSE can identify harmonic content at other buses where no observations have been made. As mentioned before, due to their capability for learning, researchers have turned to artificial intelligence technologies for HSE. While the power system parameters (impedance/admittance model) and many harmonic monitors are prerequisites for traditional HSE procedures, by utilizing AI, these needs are minimized. In [86], the harmonic current RMS values of unmonitored harmonic sources are estimated using a novel methodology, based on harmonic voltage RMS magnitudes obtained from fewer observed buses. The design of the Artificial Neural Networks (ANNs) is then refined, and harmonic current estimators based on ANNs are then created for each harmonic order and harmonic source. To further increase estimation accuracy, a novel Neural Oversampling Consensus Algorithm for Regression (NOCAR) is developed. To create NOCAR, K-Nearest Neighbor (KNN) and ANN are merged. The requirement of the network model and harmonic voltage phase angle is also removed in the proposed technique.

A harmonic impedance estimating technique is proposed in [87] based on the similarity measure algorithm and ordering points to identify the clustering structure (OPTICS). This method considers the background harmonic voltage fluctuation and utility impedance change. In the beginning, the PCC measures how comparable harmonic voltage and harmonic current are, and how the data segment with a stable background harmonic voltage will be monitored. Then, the sampled data is sorted into several clusters according to the utility impedance value using the cluster ordering diagram obtained using the OPTICS algorithm which is useful for choosing input parameters. It is worth noting that the harmonic parameters for the data from various clusters are calculated using the complex domain robust regression approach. The overall harmonic contribution is then determined using the harmonic ratio and a subjective analytic hierarchy procedure after calculating the harmonic voltage and current contributions of each harmonic. Additionally, the harmonic total contribution can be found. It should be noted that many of the approaches currently in use for determining utility harmonic impedance call for the customer side to have a substantially higher impedance than the utility side. This indicates that the proposed method is more appropriate in situations when the impedance values of the utility and customer sides are identical due to filter and reactive power compensation.

For quick and precise measurement of the fundamental, harmonics, subharmonics, interharmonics, and decaying DC components of a distorted current signal with noises, [88] introduces a novel two-fold ADALINE neural network technique. For weight vector adjustment, the secondary-ADALINE uses the least mean square (LMS) method with a fixed and big step-size. This filter plays a significant role during the training interval or transients. The primary-ADALINE, on the other hand, employs a variable step-size LMS algorithm to provide a modest steady-state error. The weights of the primary-ADALINE are adjusted in accordance with the local averages of the squared errors of both ADALINEs calculated at the end of each iteration. It is possible to

determine the desired frequency component amplitudes and phases using the weights of primary-ADALINE. By providing a separate control strategy between the steady-state error and the pace of convergence, the suggested method increases convergence speed. In the proposed design, two ADALINE modules, primary-ADALINE and secondary-ADALINE are connected in parallel when using the primary-secondary ADALINE technology. The reference signals are applied to ADALINE, which is a common parallel input, as well as to the parallel output, which is the independent collection of error signals. The fixed step-size LMS algorithm updates the coefficients of the secondary-ADALINE. A popular option is to use a big step-size value to simply accelerate convergence. This filter's coefficients are quite close to the ideal solution during training intervals or abrupt parameter changes. The primary-ADALINE, on the other hand, opts for a time variable step-size LMS algorithm to change the coefficient. The value of error magnitude drops as the algorithm approaches the steady state, resulting in a smaller step size.

A novel hybrid Quantum particle swarm optimization and Least-square (QPSO-LS) method for the real-time estimation of harmonics in noisy time-varying power data in proposed in [89]. This method features strong, reliable, and robust search capabilities as well as effective convergence properties. This technique is further verified by estimating harmonics of real-time current or voltage waveforms taken from light-emitting diode (LED) lamps and axial flux permanent magnet synchronous generators. The contributions of this study are the creation and initial use of the suggested QPSO-LS algorithm for the estimation of harmonics, such as the fundamental, integer- harmonics, interharmonics, and subharmonics of noisy power signals with various dimensionalities. The estimation of harmonic parameters is also used to assess the algorithm performance using real-time data from an axial flux permanent magnet generator (AFPMG) set-up and a LED lamp.

A different approach using the neural network technique has shown acceptable results for fast and accurate harmonic detection in noisy situations by feeding the neural network only 1/2 cycle sampled values of distorted waveforms is presented in [90], precise analyses are carried out to identify the critical elements influencing the performance effectiveness of the suggested model to achieve the lowest errors of testing patterns. Additionally, a functional neural network model has been created for identifying harmonics in waveforms that have been distorted by power lines. The network was trained using several hundred altered current waveforms, including noise examples. 1400 patterns with up to the eleventh harmonic were tested on the trained ANN model.

According to their source, harmonics in a power system can either be load harmonics or supply harmonics. The harmonic current circulating in the network is also influenced by the source impedance. As a result, the harmonic spectrum of the current reflects any change in the source impedance. Using real-world field data, [91] suggests a novel approach based on ANN to isolate and assess the influence of the source impedance change without interfering with the functioning of any load. The current for this study has a substantial number of triple harmonics. The suggested algorithm is also used to analyze the acquired data and estimate the contribution of real load harmonics at the costumer side. Based on field data acquired at a substation in Georgia, USA, this study discusses the problems associated with a utility changing its source impedance and how this affects the power system network harmonics. The test location selected is mostly a feeder for homes. Additionally, this study shows how to use neural networks to estimate a customer's actual harmonic current distortion under a certain resonance state in the distribution system.

Because they are typically the most significant ones, monitoring certain low-order harmonics in the power supply is more crucial than monitoring the entire spectrum. A method for dominating low-order harmonic estimation that is based on an adaptive wavelet neural network (AWNN) is proposed in [92]. In contrast to existing estimating techniques, which require data from at least one entire cycle, the suggested method only needs half a cycle of data points as inputs. The training method for the network parameters is a straightforward, quickly convergent, and dependable learning technique based on back propagation. The proposed AWNN method offers improved adaptability with a total of five free parameters, including input-to-output layer weights, hidden-to-output layer weights, bias, translation, and dilation. The AWNN also provides superior harmonic estimations since it uses wavelet coefficients rather than the radial distances utilized in the radial basis function neural network (RBFNN). Because wavelets are localized functions, the proposed work initializes the wavelet parameters using a rapid heuristic initialization approach, which not only shortens training time but also increases accuracy.

As we know, the power quality of modern electric networks is deteriorated due to the use of non-linear loads. When the current is not sinusoidal, it is no longer possible to calculate AC loss with the usual accuracy. On the other hand, precise calculation and prediction of the heat load generated by AC loss during the design stage are essential for the effectiveness of the cooling devices for high-power equipment. Designers of large-scale superconducting devices would therefore be very interested in the estimation of non-sinusoidal AC loss in high temperature superconducting (HTS) material. The research in [93] uses AI to predict non-sinusoidal AC loss in HTS tapes. To provide sufficient data for AI models, a 2D FE model is proposed in COMSOL Multiphysics to compute the AC loss of a typical HTS tape under current harmonics, with varying amplitude, phase angles, and harmonic contents. Second, an ANN model is utilized to estimate the non-sinusoidal AC loss for various harmonics to reduce the complexity of having a harmonic order dependent FE model for AC loss under non-sinusoidal current as well as the lengthy calculation time of the FE model.

A recurrent neural network (RNNs) with backpropagation training makes it possible to distinguish between load harmonics and supply harmonics [94]. The benefit of this method is that only voltage and current waveforms need to be measured. This study is also helpful in evaluating which side of a network (utility or customer) contributes more to harmonic pollution. This research offers a novel method based on RNN to determine the true harmonic current of a nonlinear load. The approach outlined in this paper calculates the real harmonic current distortion that a load is responsible for. Fig. 32 shows a single-line diagram of a three-phase supply network with numerous loads, one of which is nonlinear, coupled to a PCC, a sinusoidal voltage source (Vs), network impedance (Ls), and Rs. The network receives a distorted three-phase line current (i_{abc}) from the nonlinear load. To recognize the load's nonlinear features, the identification neural network (RNN1) is trained. If the load could be isolated and supplied from a pure sine supply, the estimating neural network (RNN2) predicts the distorted true harmonic current (i_{abc}) that would be injected by the load into the network. RNN2 is a structurally identical copy of the trained RNN1. It is entirely possible for RNN1 to perform the duties of RNN2 but doing so would interfere with RNN1 ongoing online training while it is estimated.

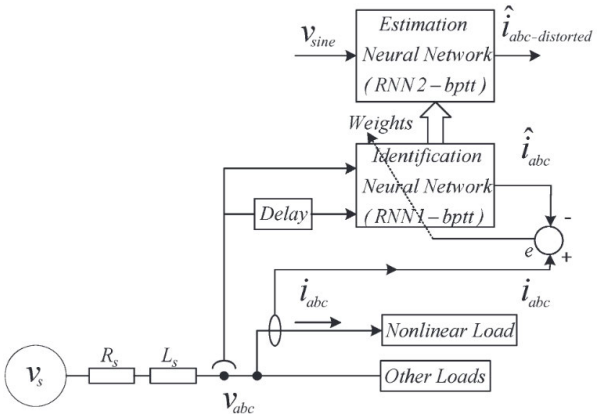

FIGURE 32. The technique proposed in [94] for estimating the true harmonic distortion.

In the underdetermined measurement system, a unique technique for estimating multi-harmonic sources has been studied in [95]. According to the suggested technique, the concept of measuring harmonics can be theoretically characterized as underdetermined matrix equations, which have an infinite number of solutions relating to all potential locations and current pollutions of the main harmonic sources. As a result of the nearly zero harmonic current emissions from non-harmonic source buses, the real number, locations, and current pollutions of harmonic sources are determined by fitting the harmonic current emissions of all potential non-harmonic source buses and selecting the case with the lowest fitting residual. To solve the minimal fitting residual of the estimated harmonic current pollutions from non-harmonic source buses, the suggested technique first finds the coefficient of a homogeneous solution for each feasible combination of suspicious harmonic sources by using a genetic algorithm. Therefore, all harmonic sources may be identified and estimated by comparing each minimal fitting residual.

VI. CONCLUSION

This paper presented a comprehensive review of harmonic estimation techniques based on traditional and Artificial Intelligence in power system networks. Harmonic mitigation techniques at the unit level and system level are investigated and different IEC and IEEE standards are studied. Although it is important to mitigate or suppress harmonic emissions in power systems, it is more crucial to estimate and predict the harmonic levels. In this case, different conventional harmonic estimation techniques are thoroughly studied. According to the review section, the conventional harmonic estimation techniques have been vastly utilized due to their association with harmonic analysis; however, they lack fast response, and accuracy, and have limited application and dependency. Therefore, Artificial Intelligence-based estimation techniques are developed as smart, efficient, and accurate alternatives due to their capability for learning, predicting, and identifying. Different Artificial Intelligence-based techniques for harmonic estimation in power networks are reviewed, which are mainly focused on machine learning, neural network, fuzzy logic, genetic algorithm, etc.

REFERENCES

[1] B. Kroposki, C. Pink, R. DeBlasio, H. Thomas, M. Simões, and P. K. Sen, "Benefits of power electronic interfaces for distributed energy systems," *IEEE Trans. Energy Convers.*, vol. 25, no. 3, pp. 901–908, Sep. 2010, doi: 10.1109/TEC.2010.2053975.

[2] Y. J. Wang, R. M. O'Connell, and G. Brownfield, "Modeling and prediction of distribution system voltage distortion caused by nonlinear residential loads," *IEEE Trans. Power Del.*, vol. 16, no. 4, pp. 744–751, Oct. 2001, doi: 10.1109/61.956765.

[3] T. D. Kefalas and A. G. Kladas, "Harmonic impact on distribution transformer no-load loss," *IEEE Trans. Ind. Electron.*, vol. 57, no. 1, pp. 193–200, Jan. 2010.

[4] X. Wang and F. Blaabjerg, "Harmonic stability in power electronic-based power systems: Concept, modeling, and analysis," *IEEE Trans. Smart Grid*, vol. 10, no. 3, pp. 2858–2870, May 2019, doi: 10.1109/TSG.2018.2812712.

[5] H. Hu, Q. Shi, Z. He, J. He, and S. Gao, "Potential harmonic resonance impacts of PV inverter filters on distribution systems," *IEEE Trans. Sustain. Energy*, vol. 6, no. 1, pp. 151–161, Jan. 2015, doi: 10.1109/TSTE.2014.2352931.

[6] P. Waide and C. Brunner, "Energy-efficiency policy opportunities for electric motor-driven systems," IEA Energy Papers, OECD Publishing, Paris, France, Tech. Rep. 2011/07, 2011, doi: 10.1787/5kgg52gb9gjd-en.

[7] A. Moradi, F. Zare, D. Kumar, J. Yaghoobi, R. Sharma, and D. Kroese, "Current harmonics generated by multiple adjustable-speed drives in distribution networks in the frequency range of 2–9 kHz," *IEEE Trans. Ind. Appl.*, vol. 58, no. 4, pp. 4744–4757, Jul. 2022, doi: 10.1109/TIA.2022.3172024.

[8] J.-S. Lai and T. S. Key, "Effectiveness of harmonic mitigation equipment for commercial office buildings," *IEEE Trans. Ind. Appl.*, vol. 33, no. 4, pp. 1104–1110, Jul. 1997, doi: 10.1109/28.605754.

[9] Y. Yang, K. Zhou, and F. Blaabjerg, "Current harmonics from single-phase grid-connected inverters-examination and suppression," *IEEE J. Emerg. Sel. Topics Power Electron.*, vol. 4, no. 1, pp. 221–233, Mar. 2016, doi: 10.1109/JESTPE.2015.2504845.

[10] S. K. Yadav, A. Patel, and H. D. Mathur, "Study on comparison of power losses between UPQC and UPQC-DG," *IEEE Trans. Ind. Appl.*, vol. 58, no. 6, pp. 7384–7395, Nov./Dec. 2022, doi: 10.1109/TIA.2022.3191985.

[11] R. N. Beres, X. Wang, F. Blaabjerg, M. Liserre, and C. L. Bak, "Optimal design of high-order passive-damped filters for grid-connected applications," *IEEE Trans. Power Electron.*, vol. 31, no. 4, pp. 2083–2098, Mar. 2016, doi: 10.1109/TPEL.2015.2441299.

[12] A. Medina-Rios and H. A. Ramos-Carranza, "An active power filter in phase coordinates for harmonic mitigation," *IEEE Trans. Power Del.*, vol. 22, no. 3, pp. 1991–1993, Jul. 2007, doi: 10.1109/TPWRD.2007.899985.

[13] P. Davari, F. Zare, and F. Blaabjerg, "Pulse pattern-modulated strategy for harmonic current components reduction in three-phase AC–DC converters," *IEEE Trans. Ind. Appl.*, vol. 52, no. 4, pp. 3182–3192, Jul. 2016, doi: 10.1109/TIA.2016.2539922.

[14] E. Hossain, M. R. Tür, S. Padmanaban, S. Ay, and I. Khan, "Analysis and mitigation of power quality issues in distributed generation systems using custom power devices," *IEEE Access*, vol. 6, pp. 16816–16833, 2018, doi: 10.1109/ACCESS.2018.2814981.

[15] H. Zhou, Y. W. Li, N. R. Zargari, G. Cheng, R. Ni, and Y. Zhang, "Selective harmonic compensation (SHC) PWM for grid-interfacing high-power converters," *IEEE Trans. Power Electron.*, vol. 29, no. 3, pp. 1118–1127, Mar. 2014, doi: 10.1109/TPEL.2013.2261553.

[16] B. Singh and P. Shukl, "Control of grid fed PV generation using infinite impulse response peak filter in distribution network," *IEEE Trans. Ind. Appl.*, vol. 56, no. 3, pp. 3079–3089, May 2020.

[17] J. F. Chicharo and H. Wang, "Power system harmonic signal estimation and retrieval for active power filter applications," *IEEE Trans. Power Electron.*, vol. 9, no. 6, pp. 580–586, Nov. 1994, doi: 10.1109/63.334772.

[18] A. P. S. Meliopoulos, F. Zhang, and S. Zelingher, "Power system harmonic state estimation," *IEEE Trans. Power Del.*, vol. 9, no. 3, pp. 1701–1709, Jul. 1994, doi: 10.1109/61.311191.

[19] P. M. Djuric and H.-T. Li, "Bayesian spectrum estimation of harmonic signals," *IEEE Signal Process. Lett.*, vol. 2, no. 11, pp. 213–215, Nov. 1995, doi: 10.1109/97.473649.

[20] H. C. Lin, "Inter-harmonic identification using group-harmonic weighting approach based on the FFT," *IEEE Trans. Power Electron.*, vol. 23, no. 3, pp. 1309–1319, May 2008.

[21] G. T. Heydt, "Identification of harmonic sources by a state estimation technique," *IEEE Trans. Power Del.*, vol. 4, no. 1, pp. 569–576, Jan. 1989, doi: 10.1109/61.19248.

[22] Z. Lu, T. Y. Ji, W. H. Tang, and Q. H. Wu, "Optimal harmonic estimation using a particle swarm optimizer," *IEEE Trans. Power Del.*, vol. 23, no. 2, pp. 1166–1174, Apr. 2008, doi: 10.1109/TPWRD.2008.917656.

[23] C. Wu, M. E. Magaña, and E. Cotilla-Sánchez, "Dynamic frequency and amplitude estimation for three-phase unbalanced power systems using the unscented Kalman filter," *IEEE Trans. Instrum. Meas.*, vol. 68, no. 9, pp. 3387–3395, Sep. 2019, doi: 10.1109/TIM.2018.2875605.

[24] D. Simon, *Optimal State Estimation: Kalman, H Infinity, and Nonlinear Approaches*. Hoboken, NJ, USA: Wiley, 2006.

[25] D. Kumar and F. Zare, "Harmonic analysis of grid connected power electronic systems in low voltage distribution networks," *IEEE Trans. Emerg. Sel. Topics Power Electron.*, vol. 4, no. 1, pp. 70–79, Mar. 2016, doi: 10.1109/JESTPE.2015.2454537.

[26] D. Heirman, "EMC standards activity," *IEEE Electromagn. Compat. Mag.*, vol. 3, no. 2, pp. 100–103, 2nd Quart., 2014.

[27] J. Yaghoobi, F. Zare, and H. Rathnayake, "Current harmonics generated by motor-side converter: New standardizations," *IEEE J. Emerg. Sel. Topics Power Electron.*, vol. 9, no. 3, pp. 2868–2880, Jun. 2021, doi: 10.1109/JESTPE.2020.3028312.

[28] *Electromagnetic Compatibility (EMC). Part 2-2: Environment. Compatibility Levels for Low-Frequency Conducted Disturbances and Signalling in Public Low-Voltage Power Supply Systems*, document I. S. 61000-2-2, 2002.

[29] *IEEE Recommended Practice and Requirements for Harmonic Control in Electric Power Systems*, Standard 519–2014 (Revision IEEE Std 519–1992), 2014, pp. 1–29, doi: 10.1109/IEEESTD.2014.6826459.

[30] D. Solatialkaran, K. G. Khajeh, and F. Zare, "A novel filter design method for grid-tied inverters," *IEEE Trans. Power Electron.*, vol. 36, no. 5, pp. 5473–5485, May 2021.

[31] K. G. Khajeh, F. Farajizadeh, D. Solatialkaran, F. Zare, J. Yaghoobi, and N. Mithulananthan, "A full-feedforward technique to mitigate the grid distortion effect on parallel grid-tied inverters," *IEEE Trans. Power Electron.*, vol. 37, no. 7, pp. 8404–8419, Jul. 2022, doi: 10.1109/TPEL.2022.3146235.

[32] E. Matijevic, R. Sharma, F. Zare, and D. Kumar, "Extremum seeking as a tool for active damping of active front-end converters," *IEEE Trans. Ind. Electron.*, vol. 70, no. 4, pp. 3404–3413, Apr. 2023, doi: 10.1109/TIE.2022.3181362.

[33] D. Solatialkaran, F. Zare, T. K. Saha, and R. Sharma, "A novel approach in filter design for grid-connected inverters used in renewable energy systems," *IEEE Trans. Sustain. Energy*, vol. 11, no. 1, pp. 154–164, Jan. 2020, doi: 10.1109/TSTE.2018.2887079.

[34] *Electromagnetic Compatibility (EMC)-Part 3–12: Limits-Limits for Harmonic Currents Produced by Equipment Connected to Public Low-Voltage Systems With Input Current> 16 A and ≤ 75 A per Phase*, I. E. Commission, International Electrotechnical Commission (IEC), Geneva, Switzerland, 2011.

[35] V. Khadkikar and A. Chandra, "A new control philosophy for a unified power quality conditioner (UPQC) to coordinate load-reactive power demand between shunt and series inverters," *IEEE Trans. Power Del.*, vol. 23, no. 4, pp. 2522–2534, Oct. 2008, doi: 10.1109/TPWRD.2008.921146.

[36] B. Singh, K. Al-Haddad, and A. Chandra, "A review of active filters for power quality improvement," *IEEE Trans. Ind. Electron.*, vol. 46, no. 5, pp. 960–971, Oct. 1999.

[37] A. Alduraibi, J. Yaghoobi, D. Solatialkaran, and F. Zare, "A modular power converter with active front-end system to mitigate harmonics in distribution networks," *IEEE J. Emerg. Sel. Topics Power Electron.*, vol. 9, no. 2, pp. 1725–1735, Apr. 2021.

[38] S. Hou, Y. Chu, and J. Fei, "Adaptive type-2 fuzzy neural network inherited terminal sliding mode control for power quality improvement," *IEEE Trans. Ind. Informat.*, vol. 17, no. 11, pp. 7564–7574, Nov. 2021.

[39] A. Moradi, J. Yaghoobi, F. Zare, and D. Kumar, "Analysis of 0–9 kHz current harmonics in a three-phase power converter under unbalanced-load conditions," *IEEE Access*, vol. 9, pp. 161862–161876, 2021, doi: 10.1109/ACCESS.2021.3131304.

[40] A. Moradi, J. Yaghoobi, and F. Zare, "A precise model of DC-link current in adjustable speed drives for the harmonic analysis of electrical networks," *IEEE Access*, vol. 10, pp. 45663–45676, 2022, doi: 10.1109/ACCESS.2022.3170412.

[41] W. Zhou, O. Ardakanian, H.-T. Zhang, and Y. Yuan, "Bayesian learning-based harmonic state estimation in distribution systems with smart meter and DPMU data," *IEEE Trans. Smart Grid*, vol. 11, no. 1, pp. 832–845, Jan. 2020.

[42] C. Rakpenthai, S. Uatrongjit, N. R. Watson, and S. Premrudeepreechacharn, "On harmonic state estimation of power system with uncertain network parameters," *IEEE Trans. Power Syst.*, vol. 28, no. 4, pp. 4829–4838, Nov. 2013.

[43] D. Carta, C. Muscas, P. A. Pegoraro, A. V. Solinas, and S. Sulis, "Compressive sensing-based harmonic sources identification in smart grids," *IEEE Trans. Instrum. Meas.*, vol. 70, pp. 1–10, 2021.

[44] X. Xiao, Z. Li, Y. Wang, and Y. Zhou, "A practical approach to estimate harmonic distortions in residential distribution system," *IEEE Trans. Power Del.*, vol. 36, no. 3, pp. 1418–1427, Jun. 2021.

[45] R. A. S. Fernandes, M. Oleskovicz, and I. N. da Silva, "Harmonic source location and identification in radial distribution feeders: An approach based on particle swarm optimization algorithm," *IEEE Trans. Ind. Informat.*, vol. 18, no. 5, pp. 3171–3179, May 2022, doi: 10.1109/TII.2021.3108681.

[46] G. D'Antona, C. Muscas, and S. Sulis, "State estimation for the localization of harmonic sources in electric distribution systems," *IEEE Trans. Instrum. Meas.*, vol. 58, no. 5, pp. 1462–1470, May 2009, doi: 10.1109/TIM.2009.2014504.

[47] G. D'Antona, C. Muscas, and S. Sulis, "Localization of nonlinear loads in electric systems through harmonic source estimation," *IEEE Trans. Instrum. Meas.*, vol. 60, no. 10, pp. 3423–3430, Oct. 2011, doi: 10.1109/TIM.2011.2126830.

[48] G. D'Antona, C. Muscas, P. A. Pegoraro, and S. Sulis, "Harmonic source estimation in distribution systems," *IEEE Trans. Instrum. Meas.*, vol. 60, no. 10, pp. 3351–3359, Oct. 2011, doi: 10.1109/TIM.2011.2126910.

[49] R. A. Wiltshire, G. Ledwich, and P. O'Shea, "A Kalman filtering approach to rapidly detecting modal changes in power systems," *IEEE Trans. Power Syst.*, vol. 22, no. 4, pp. 1698–1706, Nov. 2007.

[50] J. P. Muñoz, M. E. Magaña, and E. Cotilla-Sanchez, "Adaptive master–slave unscented Kalman filter for grid voltage frequency estimation," *IET Signal Process.*, vol. 12, no. 4, pp. 496–505, Jun. 2018.

[51] A. Elrayyah, A. Safayet, Y. Sozer, I. Husain, and M. Elbuluk, "Efficient harmonic and phase estimator for single-phase grid-connected renewable energy systems," *IEEE Trans. Ind. Appl.*, vol. 50, no. 1, pp. 620–630, Jan./Feb. 2014.

[52] H. Wen, J. Zhang, Z. Meng, S. Guo, F. Li, and Y. Yang, "Harmonic estimation using symmetrical interpolation FFT based on triangular self-convolution window," *IEEE Trans. Ind. Informat.*, vol. 11, no. 1, pp. 16–26, Feb. 2015.

[53] J. Yong, L. Chen, and S. Chen, "Modeling of home appliances for power distribution system harmonic analysis," *IEEE Trans. Power Del.*, vol. 25, no. 4, pp. 3147–3155, Oct. 2010.

[54] C. M. Hackl and M. Landerer, "Modified second-order generalized integrators with modified frequency locked loop for fast harmonics estimation of distorted single-phase signals," *IEEE Trans. Power Electron.*, vol. 35, no. 3, pp. 3298–3309, Mar. 2020.

[55] R. R. Aleixo, T. S. Lomar, L. R. M. Silva, H. L. M. Monteiro, and C. A. Duque, "Real-time B-spline interpolation for harmonic phasor estimation in power systems," *IEEE Trans. Instrum. Meas.*, vol. 71, pp. 1–9, 2022.

[56] J. Sun, E. Aboutanios, D. B. Smith, and J. E. Fletcher, "Robust frequency, phase, and amplitude estimation in power systems considering harmonics," *IEEE Trans. Power Del.*, vol. 35, no. 3, pp. 1158–1168, Jun. 2020.

[57] E. Sezgin, M. Gol, and O. Salor, "State estimation based determination of harmonic current contributions of iron and steel plants supplied from PCC," in *Proc. IEEE Ind. Appl. Soc. Annu. Meeting*, Oct. 2015, pp. 1–10.

[58] C. F. M. Almeida and N. Kagan, "Harmonic state estimation through optimal monitoring systems," *IEEE Trans. Smart Grid*, vol. 4, no. 1, pp. 467–478, Mar. 2013.

[59] E. F. de Arruda, N. Kagan, and P. F. Ribeiro, "Harmonic distortion state estimation using an evolutionary strategy," *IEEE Trans. Power Del.*, vol. 25, no. 2, pp. 831–842, Apr. 2010.

[60] Z. Dai and W. Lin, "Adaptive estimation of three-phase grid voltage parameters under unbalanced faults and harmonic disturbances," *IEEE Trans. Power Electron.*, vol. 32, no. 7, pp. 5613–5627, Jul. 2017.

[61] Z. Shuai, J. Zhang, L. Tang, Z. Teng, and H. Wen, "Frequency shifting and filtering algorithm for power system harmonic estimation," *IEEE Trans. Ind. Informat.*, vol. 15, no. 3, pp. 1554–1565, Mar. 2019.

[62] L. Chen, W. Zhao, X. Xie, D. Zhao, and S. Huang, "Harmonic phasor estimation based on frequency-domain sampling theorem," *IEEE Trans. Instrum. Meas.*, vol. 70, pp. 1–10, 2021.

[63] F. Ornelas-Tellez, J. J. Rico-Melgoza, R. Morfin-Magana, and S. Ramos-Paz, "Optimal dynamic harmonic extraction and suppression in power conditioning applications," *IEEE Trans. Ind. Electron.*, vol. 67, no. 9, pp. 7909–7918, Sep. 2020.

[64] H. Xue, M. Wang, R. Yang, and Y. Zhang, "Power system frequency estimation method in the presence of harmonics," *IEEE Trans. Instrum. Meas.*, vol. 65, no. 1, pp. 56–69, Jan. 2016.

[65] S. Vieira, W. H. L. Pinaya, and A. Mechelli, "Introduction to machine learning," in *Machine Learning*. Amsterdam, The Netherlands: Elsevier, 2020, pp. 1–20.

[66] Y. Roh, G. Heo, and S. E. Whang, "A survey on data collection for machine learning: A big data-AI integration perspective," *IEEE Trans. Knowl. Data Eng.*, vol. 33, no. 4, pp. 1328–1347, Apr. 2019.

[67] Y. Wang, Y. Li, Y. Song, and X. Rong, "The influence of the activation function in a convolution neural network model of facial expression recognition," *Appl. Sci.*, vol. 10, no. 5, p. 1897, Mar. 2020.

[68] H. Zhang, T.-W. Weng, P.-Y. Chen, C.-J. Hsieh, and L. Daniel, "Efficient neural network robustness certification with general activation functions," in *Proc. Adv. Neural Inf. Process. Syst.*, vol. 31, 2018, pp. 1–10.

[69] Y. Ho and S. Wookey, "The real-world-weight cross-entropy loss function: Modeling the costs of mislabeling," *IEEE Access*, vol. 8, pp. 4806–4813, 2020.

[70] A. Lucas, S. López-Tapia, R. Molina, and A. K. Katsaggelos, "Generative adversarial networks and perceptual losses for video super-resolution," *IEEE Trans. Image Process.*, vol. 28, no. 7, pp. 3312–3327, Jul. 2019.

[71] M. Raissi, Z. Wang, M. S. Triantafyllou, and G. E. Karniadakis, "Deep learning of vortex-induced vibrations," *J. Fluid Mech.*, vol. 861, pp. 119–137, Feb. 2019.

[72] D. P. Kingma and J. Ba, "Adam: A method for stochastic optimization," 2014, *arXiv:1412.6980*.

[73] S. Ruder, "An overview of gradient descent optimization algorithms," 2016, *arXiv:1609.04747*.

[74] H. Robbins and S. Monro, "A stochastic approximation method," *Ann. Math. Statist.*, vol. 22, no. 3, pp. 400–407, 1951.

[75] Y. Bengio, P. Simard, and P. Frasconi, "Learning long-term dependencies with gradient descent is difficult," *IEEE Trans. Neural Netw.*, vol. 5, no. 2, pp. 157–166, Mar. 1994.

[76] S. Hochreiter and J. Schmidhuber, "Long short-term memory," *Neural Comput.*, vol. 9, no. 8, pp. 1735–1780, 1997.

[77] T. Fernando, H. Gammulle, S. Denman, S. Sridharan, and C. Fookes, "Deep learning for medical anomaly detection-a survey," *ACM Comput. Surv.*, vol. 54, no. 7, pp. 1–37, 2021.

[78] T. Fernando, S. Sridharan, S. Denman, H. Ghaemmaghami, and C. Fookes, "Robust and interpretable temporal convolution network for event detection in lung sound recordings," *IEEE J. Biomed. Health Informat.*, vol. 26, no. 7, pp. 2898–2908, Jul. 2022.

[79] J. Luo, H. Qiao, and B. Zhang, "Learning with smooth Hinge losses," *Neurocomputing*, vol. 463, pp. 379–387, Nov. 2021.

[80] H. R. Baghaee, D. Mlakic, S. Nikolovski, and T. Dragicevic, "Support vector machine-based islanding and grid fault detection in active distribution networks," *IEEE J. Emerg. Sel. Topics Power Electron.*, vol. 8, no. 3, pp. 2385–2403, Sep. 2020.

[81] S. Katyara, L. Staszewski, and Z. Leonowicz, "Signal parameter estimation and classification using mixed supervised and unsupervised machine learning approaches," *IEEE Access*, vol. 8, pp. 92754–92764, 2020.

[82] A. Zebardast and H. Mokhtari, "New method for assessing the utility harmonic impedance based on fuzzy logic," *IET Gener., Transmiss. Distrib.*, vol. 11, no. 10, pp. 2448–2456, Jul. 2017.

[83] S. K. Jain, S. N. Singh, and J. G. Singh, "An adaptive time-efficient technique for harmonic estimation of nonstationary signals," *IEEE Trans. Ind. Electron.*, vol. 60, no. 8, pp. 3295–3303, Aug. 2013.

[84] S. K. Jain and S. N. Singh, "Exact model order ESPRIT technique for harmonics and interharmonics estimation," *IEEE Trans. Instrum. Meas.*, vol. 61, no. 7, pp. 1915–1923, Jul. 2012.

[85] S. K. Jain and S. N. Singh, "Fast harmonic estimation of stationary and time-varying signals using EA-AWNN," *IEEE Trans. Instrum. Meas.*, vol. 62, no. 2, pp. 335–343, Feb. 2013.

[86] A. Eslami, M. Negnevitsky, E. Franklin, and S. Lyden, "Harmonic current estimation of unmonitored harmonic sources with a novel oversampling technique for limited datasets," *IEEE Access*, vol. 10, pp. 68897–68914, 2022.

[87] Z. Liu, Y. Xu, H. Jiang, and S. Tao, "Study on harmonic impedance estimation and harmonic contribution evaluation index," *IEEE Access*, vol. 8, pp. 59114–59125, 2020.

[88] P. Garanayak, R. T. Naayagi, and G. Panda, "A high-speed master-slave ADALINE for accurate power system harmonic and inter-harmonic estimation," *IEEE Access*, vol. 8, pp. 51918–51932, 2020.

[89] A. B. Waqas, M. M. Ashraf, and Y. Saifullah, "A hybrid quantum inspired particle swarm optimization and least square framework for real-time harmonic estimation," *J. Modern Power Syst. Clean Energy*, vol. 9, no. 6, pp. 1548–1556, 2021.

[90] H. C. Lin, "Intelligent neural network-based fast power system harmonic detection," *IEEE Trans. Ind. Electron.*, vol. 54, no. 1, pp. 43–52, Feb. 2007.

[91] J. Mazumdar, R. G. Harley, F. C. Lambert, G. K. Venayagamoorthy, and M. L. Page, "Intelligent tool for determining the true harmoniccurrent contribution of a customer in a power distribution network," *IEEE Trans. Ind. Appl.*, vol. 44, no. 5, pp. 1477–1485, Sep./Oct. 2008.

[92] S. K. Jain and S. N. Singh, "Low-order dominant harmonic estimation using adaptive wavelet neural network," *IEEE Trans. Ind. Electron.*, vol. 61, no. 1, pp. 428–435, Jan. 2014.

[93] M. Yazdani-Asrami, M. Taghipour-Gorjikolaie, W. Song, M. Zhang, and W. Yuan, "Prediction of nonsinusoidal AC loss of superconducting tapes using artificial intelligence-based models," *IEEE Access*, vol. 8, pp. 207287–207297, 2020.

[94] J. Mazumdar and R. G. Harley, "Recurrent neural networks trained with backpropagation through time algorithm to estimate nonlinear load harmonic currents," *IEEE Trans. Ind. Electron.*, vol. 55, no. 9, pp. 3484–3491, Sep. 2008.

[95] F. Xu, C. Wang, K. Guo, Q. Shu, Z. Ma, and H. Zheng, "Harmonic sources' location and emission estimation in underdetermined measurement system," *IEEE Trans. Instrum. Meas.*, vol. 70, pp. 1–11, 2021.

AMIR TAGHVAIE (Member, IEEE) was born in Sari, Iran, 1990. He received the M.Eng. degree in electrical power engineering from Babol Noshirvani University of Technology, Babol, Iran, in 2016, and the Ph.D. degree in electrical power engineering from Deakin University, Geelong, VIC, Australia, in 2021. He was a Research Fellow with The University of Queensland, Brisbane, QLD, Australia, in 2022, where he is currently a Research Fellow with the School of Electrical Engineering and Robotics. His research interests include design of power electronics converters, power quality, pulsed power, switched capacitor converters, and renewable energy.

T. WARNAKULASURIYA (Member, IEEE) is a Research Fellow with the Signal Processing, Artificial Intelligence, and Vision Technologies (SAIVT) Research Program, School of Electrical Engineering and Robotics, Queensland University of Technology (QUT). After his Ph.D., he was conducting interdisciplinary research activities and collaborating with researchers in healthcare, neuroscience, psychology, and computer vision to solve challenging problems in several domains. His research interests include artificial intelligence, computer vision, deep learning, bio signal processing, and video analytics. He was a recipient of the 2019 QUT University Award for Outstanding Doctoral Thesis and the QUT Early Career Researcher Award in 2022.

DINESH KUMAR (Senior Member, IEEE) received the M.Tech. degree in power system engineering from the Indian Institute of Technology (IIT), Roorkee, India, in 2004, and the Ph.D. degree in power electronics from the University of Nottingham, U.K., in 2010. From 2004 to 2005, he was a Lecturer with the Electrical Engineering Department, National Institute of Technology, Kurukshetra, India. In 2006, he joined Technical University Chemnitz, Germany, as a Research Fellow in power electronics. Since 2011, he has been with Danfoss Drives A/S, Denmark, where he is involved in many research and industrial projects. He is an Adjunct Associate Professor with the School of Electrical Engineering and Robotics, Faculty of Engineering, Queensland University of Technology, Australia. His current research interests include motor drive, harmonic analysis and mitigation techniques, and power quality and electromagnetic interference in power electronics. He is a member of the IEC standardization Working Group in TC77A, TC22/SC22G, and SyC LVDC Committee. He was a recipient of two IEEE best paper awards. He is the Editor-in-Chief of *International Journal of Power Electronics*, an Associate Editor of IEEE TRANSACTIONS ON INDUSTRY APPLICATIONS, IEEE ACCESS journal, and a member of Editorial Board of IEEE TRANSPORTATION ELECTRIFICATION eNEWSLETTER.

FIRUZ ZARE (Fellow, IEEE) is a fellow of Engineers Australia, an IEEE Distinguished Lecturer, and the Head of School of Electrical Engineering and Robotics, Queensland University of Technology, Australia. He has over 20 years of experience in academia, industry, and international standardization committees, including eight years in two large research and development centers in Denmark, working on grid connected inverters, energy conversion systems, and power quality projects. He was an active member of IEC, Danish, and the Australian Standardization Committees. He was a Task Force Leader (International Project Manager) of Active Infeed Converters to develop the first international standard IEC 61000-3-16 within the IEC standardization SC77A. He has published over 300 peer-reviewed conference and journal papers including four books and supervised over 20 Ph.D. students, postdocs, and research engineers. His research interests include advanced power converter topology and control in grid connected renewable energy, motor drives and energy storage systems, electromagnetic interferences and harmonics in power systems, addressing standardization and emerging issues of future grids, and pulsed power systems for bioelectric and industrial applications. He received several awards, such as the Australian Future Fellowship, the John Madsen Medal, the Symposium Fellowship, and the Early Career Excellence Research Award. He is a Senior Editor of IEEE ACCESS journal, a Guest Editor and an Associate Editor of the IEEE JOURNAL OF EMERGING AND SELECTED TOPICS IN POWER ELECTRONICS, and an editorial board member of several international journals.

RAHUL SHARMA (Senior Member, IEEE) received the Master of Engineering Science and Ph.D. degrees in electrical engineering from the University of Melbourne, Melbourne, VIC, Australia. He is currently a Senior Lecturer with the School of Information Technology and Electrical Engineering, The University of Queensland, Brisbane, QLD, Australia. His research interests include control theory development and applications to control of grid connected inverters, demand management algorithms, and monitoring of large solar farms. He was a recipient of the SAE-A Young Engineer of the Year Award in 2010 and number of industry and academia selected best paper awards.

D. MAHINDA VILATHGAMUWA (Fellow, IEEE) received the Ph.D. degree from the University of Cambridge, U.K. He is a Professor of power engineering with the Queensland University of Technology, Brisbane, Australia. His research interests include battery modeling and control, power electronics, wireless power transfer, and electromobility.